Journal Pre-proof

Breaking the classics: Next-generation biosensors for the isolation, profiling and detection of extracellular vesicles

Raquel Vaz, Verónica M. Serrano, Yuselis Castaño-Guerrero, Ana R. Cardoso, Manuela F. Frasco, M. Goreti F. Sales

Please cite this article as: Vaz, R., Serrano, Veró.M., Castaño-Guerrero, Y., Cardoso, A.R., Frasco, M.F., Sales, M.G.F., Breaking the classics: Next-generation biosensors for the isolation, profiling and detection of extracellular vesicles, *Biosensors and Bioelectronics: X* (2022), doi: https://doi.org/10.1016/j.biosx.2022.100115.

Breaking the classics: next-generation biosensors for the isolation, profiling and detection of extracellular vesicles

Raquel Vaz[1,3,4], Verónica M. Serrano[1,3,4], Yuselis Castaño-Guerrero[2,3,4], Ana R. Cardoso[2,3,4], Manuela F. Frasco[1,2,3,4]* and M. Goreti F. Sales[1,2,3,4]*

[1]*BioMark@UC, Faculty of Sciences and Technology, Coimbra University, Coimbra, Portugal*

[2]*BioMark@ISEP, School of Engineering, Polytechnic Institute of Porto, Porto, Portugal*

[3]*CEB – Centre of Biological Engineering, Minho University, Braga, Portugal*

[4]*LABBELS – Associate Laboratory, Braga, Guimarães, Portugal*

*To whom correspondence should be addressed. Email addresses: mffrasco@gmail.com (MF Frasco) and/or goreti.sales@eq.uc.pt/goreti.sales@gmail.com (MGF Sales).

Abstract

Extracellular vesicles (EVs) contain biomarkers that may represent a paradigm shift in timely disease diagnosis and personalized therapeutic approaches. Despite tremendous progress in this field, the considerable complexity and heterogeneity of EVs, combined with hurdles in isolation and accurate characterization, have delayed their envisioned clinical translation. At the same time, emerging biosensor technologies are trying to overcome the limitations and provide new momentum to EVs research. In this review, the focus is given on the variety of novel approaches to improve the capture of EVs of interest from a myriad of sample types in terms of yield, purity, sensitivity, and specificity. These biosensing devices also contribute to the understanding of the content of EVs in correlation with their function. Given the pivotal role of EVs uncovered to date and the recent technological advances discussed herein, nanosensing platforms offer low-cost, fast, simple, and accurate methods that are likely to help gain more insight into the biology of EVs. Moreover, the prospect of identifying new roles and patterns will reinforce the importance of EVs and intercellular communication in health status.

Keywords: extracellular vesicles, intercellular communication, biosensors, nanotechnology, health monitoring

1. Introduction

Historically, intercellular communication was considered to occur through soluble factors mainly via three routes: autocrine, an autonomous regulatory process because the target cell is the secreting cell; paracrine, when the target cell is near the secreting cell; and endocrine, when cells communicate remotely via soluble factors in the blood (Yanez-Mo et al. 2015). The discovery of the new pathway via the release of membrane-enclosed particles called extracellular vesicles (EVs) has revolutionized the field (Minciacchi et al. 2015).

EVs is a general term that does not distinguish membrane particles regarding size, density, biogenesis, function, and molecular cargo. EVs are formed by lipid curvature to an inward budding vesicle within the endocytic system or to an outward budding vesicle at the plasma membrane. In the first case, exosomes are formed and are smaller than 150 nm, whereas in the second case, microvesicles or ectosomes are formed and range in size from 100 nm to 1 µm (Doyle and Wang 2019). Cancer cells produce even larger EVs, called large oncosomes (1-10 µm), also from the cell membrane (Maas et al. 2017). There are also apoptotic bodies, which are formed during apoptosis of the cell, are variable in size, and are difficult to distinguish from other EVs (Maas et al. 2017). A detailed description of the biogenesis of EVs is beyond the scope of this review and can be found elsewhere (Colombo et al. 2014; Frankel and Audhya 2018; Horner et al. 2018; van Niel et al. 2018).

EVs are found in biological fluids (e.g., blood, urine, saliva, breast milk, amniotic fluid, sperm, cerebrospinal fluid, and synovial fluid) and are considered to store important information in their content of nucleic acids, proteins, and lipids (Chiriaco et al. 2018). Communication occurs through delivery of the EVs cargo to recipient cells by cell fusion with the membrane of the target cell (Bunggulawa et al. 2018). The composition of EVs is complex and consists of various combinations of proteins, lipids, DNA, non-coding RNA, small nucleolar RNA, mitochondrial RNA, vault RNA and fragmented mRNA (Maas et al. 2017). The composition of EVs closely reflects their biogenesis and the physiological conditions of the cell of origin. For example, the membranes of EVs are usually enriched in lipid rafts (e.g., GM1 gangliosides, cholesterol,

sphingomyelin), endosome-specific proteins, and tetraspanins (e.g., CD9, CD63, CD81) (Chiriaco et al. 2018). EVs are involved not only in physiological but also in pathological processes. Understanding the function of EVs concerns the fate of their components and the biochemical changes they induce in recipient cells. For example, they can promote tumorigenesis (Melo et al. 2014), chemotaxis for immune defence, wound healing, and cancer cell migration and invasion (Kulkarni et al. 2019; Soung et al. 2016; Sung and Weaver 2017). They also influence immunological responses (Du et al. 2020; Rojas et al. 2020), neuroinflammation and neurogenesis (Yang et al. 2017), neurodegenerative diseases (Aharon et al. 2020; Groen et al. 2020), and physiological development (Baci et al. 2020; Guay et al. 2020; Nakamura et al. 2020). The relevance of EVs as health status players is also an opportunity to develop new drug delivery vehicles and nanotherapeutics (Fig. 1A).

A major focus in the analysis of EVs is their isolation and simultaneous characterization of cell surface biomarkers. Ultracentrifugation, ultrafiltration, immunoaffinity, polymer sedimentation and size exclusion chromatography, are the most commonly used techniques in current research settings (Kurian et al. 2021) (Fig. 1B). The major limitation in isolation techniques is the final purity of EVs subpopulations. This is first related to their size, which is within the size of many other contaminants, such as lipids, small organelles, microparticles, immune complexes, and calcium-phosphate microprecipitates, among others, which can cause artifacts (Gurunathan et al. 2019; van der Pol et al. 2016). In addition, individual classes of EVs are very difficult to distinguish because of overlapping size, density, and cargo (Reiner et al. 2017b; van der Pol et al. 2016). Each isolation technique takes advantage of a specific property of EVs, such as density, size, or surface biomarkers. In the absence of an optimal isolation method and depending on the level of recovery versus specificity sought, most researchers use a combination of methods. According to the International Society for Extracellular Vesicles (ISEV) position statements, MISEV2014 guidelines (Lotvall et al. 2014), updated in MISEV2018 (Thery et al. 2018), researchers in this field should follow the stated recommendations for separation and enrichment of EVs, and providing all technical details is critical for reproducibility (Thery et al. 2018).

To address the problem of EVs heterogeneity and to make their future application in clinical practice a reality, another step is crucial: optimization and standardization of the methodology for EVs identification and increasing understanding of their cargo and role (Rupert et al. 2017; Sunkara et al. 2016). The ISEV in their position statements has recommended several methods for EVs analysis (Lotvall et al. 2014; Thery et al. 2018). Among the different techniques, the common choices are the imaging methods based on electron microscopy, namely transmission electron microscopy (TEM), including cryo-TEM (Rupert et al. 2017). Other techniques widely used in the characterization of nanomaterials have proved their value also for studying EVs (Fig. 1C). Beyond the physical characterization, determining the cell/tissue type that gave origin to certain EVs is relevant to understand the etiology of diseases and the role of EVs in disease-communication (Stahl and Raposo 2018). Thus, by studying the antigens on the surface of EVs and its cargo, one can gain useful information on the cell of origin (Mathieu et al. 2019). Considering the guidelines of MISEV2018, the presence of EVs should be demonstrated by at least three positive protein markers, including detection of at least one transmembrane protein (e.g., CD63, CD81, integrins), and one cytosolic protein (e.g., TSG101, ALIX) (Thery et al. 2018). Moreover, another recommendation regards the quantification of contaminants co-isolated with EVs as purity controls, especially relevant when analysing EVs from biofluids. The analysis of lipoproteins, albumin, uromodulin, among others is then useful to determine the purity of EVs. The main methods to analyse the biochemical profile of EVs regarding their protein content are western blotting, immunosorbent assays, mass spectrometry and flow cytometry (Hartjes et al. 2019; Linares et al. 2017; Shao et al. 2018). In addition to their protein composition, EVs also enclose relevant genetic information, including both DNA and RNA. EVs nucleic acids have been extensively researched, especially as disease biomarkers (Momen-Heravi et al. 2018). For analysing RNA content next-generation sequencing of nucleic acids and microarray platforms have been developed (Everaert et al. 2019; Giraldez et al. 2019; Hrdlickova et al. 2017; Trivedi and Abreu 2018; Xu et al. 2019; Zhou et al. 2019b). As subjects of great relevance in the study of EVs, thorough reading on EVs quantification, characterization, and comparison of efficiency

among the classical characterization methods can be found elsewhere (Coumans et al. 2017; Lennon et al. 2019; Maas et al. 2015; van der Pol et al. 2014).

As mentioned, effective isolation of EVs and various subsets from biological fluids is a critical step for studying their physicochemical composition, mechanisms of action, cargo content, disease-associated biomarkers, and application in clinical and laboratory contexts, either for therapeutics or monitoring/detection. However, classical analytical methods have several downsides, like the need for high-cost instruments that are usually difficult to operate and calibrate, as well as frequent inaccuracy, lack of reliable results, and the inability to analyse EVs directly in complex matrices (Yildizhan et al. 2021). These difficulties emphasise the need to develop next-generation biosensors. Recent literature points out a significant trend towards the adaptation of the classical techniques of isolation, quantification, and characterization of EVs to unique miniaturized biosensors. Particularly addressed in this review are the new interesting microfluidic designs, reducing sample volume analysis, while improving the precision of the isolation step. The integration of microfluidics with biosensor technology has also been explored, but most studies herein described confirm that biosensors application in the field of EVs go beyond the expectations to demonstrate their selectivity and sensitivity in detection and quantification. Finally, future trends for further innovation and application in biomedicine and clinical translation are summarized.

2. Microfluidic approaches for isolation of EVs

Although many approaches have been developed for EVs isolation from biofluids, most of them have substantial shortcomings including long processing time, high cost and surface marker dependency for showing selectivity (Shi et al. 2019). Moreover, most EVs belong to nanoscale and are encountered in complex biological fluids, which make them difficult to separate and characterize. The classical techniques for isolation reflect difficulty at maintaining the vesicles intact, and purity is usually not obtained, showing heterogeneous EVs populations. Thus, characterization results in average properties of different particles. To address these limitations,

microfluidic devices have been designed and proved successful at using small sample volumes, while obtaining high purity products (Santana et al. 2014). They have the advantage of being miniaturized, thus accomplishing EVs isolation with low volume, low cost, simplicity and retaining EVs morphology (Liga et al. 2015). Moreover, isolation and profiling of EVs can be combined on a single device, reducing the workload (Stam et al. 2021).

Generally, microfluidics applied to EV analyses fall into two main approaches: using specific markers in immunoaffinity capture (Chen et al. 2010; Dudani et al. 2015; Hisey et al. 2018; Kamyabi et al. 2020; Lo et al. 2020; Reategui et al. 2018; Sun et al. 2020; Tayebi et al. 2020), or separation based on size and density of EVs. This last process encompasses acoustofluidic (Broman et al. 2021; Lee et al. 2015b; Mirtaheri et al. 2019; Wang et al. 2020f; Wu et al. 2019; Wu et al. 2017), electrophoretic (Cho et al. 2016; Davies et al. 2012; Guo et al. 2020; Guzman and Guzman 2020; Kato et al. 2013; Lee et al. 2020; Morani et al. 2020; Ouahabi et al. 2021; Shi et al. 2019), nanowire trapping (Chen et al. 2018; Dong et al. 2019a; Suwatthanarak et al. 2021; Wang et al. 2013; Yasui et al. 2017), lateral displacement (Biagioni et al. 2020; Hattori et al. 2019; Laki et al. 2014; Salafi et al. 2019; Santana et al. 2014; Smith et al. 2018; Wunsch et al. 2016) or viscoelastic flow (Asghari et al. 2020; Liu et al. 2017; Liu et al. 2019) based devices.

2.1. Immunoaffinity-based separation microfluidics

EVs separation by immunoaffinity involves the immobilization of antibodies on the microfluidic surface. There are several examples on the literature, as it is the case of Chen et al. (2010), who isolated EVs from cell culture, as well as from serum and blood samples. For that, the research team constructed a microfluidic device with planar flow channels with herringbone engravings. The herringbone engravings enhanced mixing of particles and capture efficiency, due to increased surface area. The microchannels were then functionalized with anti-CD63 (Chen et al. 2010). Dudani et al. (2015) constructed a microfluidic device on polydimethylsiloxane (PDMS) by photolithography, and polystyrene beads functionalized with anti-CD63 that were pre-incubated with the samples. Then, the exosome-bead complexes were injected in the microfluidic device, which rapidly purified exosomes through inertial force-induced solution

7

exchange. However, this method required a centrifugation step prior to the use of the device (Dudani et al. 2015). Kamyabi et al. (2020) also developed a microfluidic device functionalized with antibodies against EV surface proteins (CD9, CD63, CD81 and Epithelial Cell Adhesion Molecule [EpCAM]), but with thousands of pillars in a zigzag pattern to influence sample flow and increase interaction between the pillars and EVs for efficient screening of samples from pancreatic cancer patients (Kamyabi et al. 2020). Tayebi et al. (2020) produced such efficient trapping arrays that were able to trap one single microbead per site. Each bead was enriched with exosomes by immunoaffinity capture (Tayebi et al. 2020) (Fig. 2).

The step of realising the capture of intact EVs remains a challenge, but it has been proven that using low pH buffer, neutralized downstream, is effective and ensures EVs stability (Hisey et al. 2018). Other approaches avoid using conditions outside the physiological range. For example, EVs were captured by desthiobiotin-conjugated antibodies, which were able to connect to the device surface functionalized with Neutravidin. By adding a biotin solution, which presents higher binding affinity than the antibodies, the EVs were released from the device (Lo et al. 2020). Sun et al. (2020) built the EV Click Chip, where click chemistry motifs (tetrazine and trans-cyclooctene) were grafted onto EVs and the chip substrate, which resulted into covalent capture. Then, release was allowed by exposure to a disulphide cleavage agent (Sun et al. 2020).

2.2. Physical-based separation microfluidics

2.2.1. Acoustofluidics

Acoustics-based microfluidics usually resort to ultrasound waves to create pressure. Since particles have different mechanical properties (size, density, compressibility), they also experience differential forces (Shao et al. 2018). Wu et al. (2017) isolated exosomes directly from blood using a microfluidic device combined with acoustics. The platform consisted of two sequential surface acoustic wave (SAW) microfluidic modules: the first one removed large blood components, whereas the second one isolated exosomes with a purity of 98.4%. Each module had

a tilted-angle standing SAW field that induced lateral deflection and size-based separation. Thus, by adjusting the input power and frequency as well as the fluid flow rate, it was possible to ensure proper cut-off size of the particles of interest (Wu et al. 2017). Wu et al. (2019) were also able to use acoustofluidics to separate lipoproteins from EVs. For that, two series of SAWs were generated and propagated in opposite directions, resulting in regions of minimal pressure (pressure nodes) and regions of maximum pressure (antinodes). Whereas high-density lipoproteins and EVs tend to move to acoustic pressure modes, the remaining lipoproteins move to the antinodes. Even though EVs are not totally separated from all lipoproteins, the device is able to ameliorate the EVs isolation from biological samples (Wu et al. 2019).

Mirtaheri et al. (2019) used synthetic vesicles to study the combination of temperature and acoustic waves. The vesicles had different membrane protein content. By applying a specific temperature, conformational changes occurred on the membrane, leading to acoustic properties change. Therefore, vesicle migration shifted from the nodal to the antinodal plane according to the content. This way, vesicles containing the same proteins with different concentrations could be differentiated (Mirtaheri et al. 2019). Broman et al. (2021) reported an acoustic trapping device with a glass capillary larger than the ones reported in other studies, which allowed increasing the capacity of the device, besides enabling higher flow rates without increasing shear stress on the vesicles. Furthermore, nine trapping nodes were generated, demonstrating fast separation of EVs with distinct proteome patterns from urine samples (Broman et al. 2021).

2.2.2. Electrophoretic-based devices

Capillary electrophoresis is a high-performance electroseparation technique that isolates analytes in a capillary tube, under the influence of an electric field. The separation is based on the charge-to-hydrodynamic radius ratio of the analyte (Ouahabi et al. 2021). Compared to traditional electrophoresis devices, microcapillary electrophoresis enables reliable measurements of electrokinetic properties, such as the zeta potential and electrophoretic movement, since the electroosmotic flow in a capillary is a simple plug flow instead of a complex vortex flow. Furthermore, microcapillary electrophoresis is compatible with microscopic imaging, being a

powerful tool for particles profiling (Kato et al. 2013). For example, it is possible to attain the electrophoretic multiwavelength profile of previously prepared enriched exosomes samples (Ouahabi et al. 2021). Moreover, the zeta potential (which is based on the electrophoretic mobility) can also be used to distinguish the exosomes' cells of origin, since exosomes from cancer cells have a negative shift on zeta potential distribution in comparison to the ones resulting from normal cells (Kato et al. 2013).

Davies et al. (2012) designed a strategy to sieve EVs directly from blood, by imposing the sample through nanoporous membranes using pressure. Photopatterned porous polymer monoliths, used as filter membrane, removed cells and large debris from blood, allowing small vesicles to pass. Then, electrophoresis was applied to isolate EVs from soluble proteins since they show differences in mobility. However, the process showed to be lengthy (Davies et al. 2012). Cho et al. (2016) used a similar strategy, but with a dialysis membrane with 30 nm pores. By applying an electric field, proteins migrated through it, whereas EVs stayed on the membrane surface. In 30 minutes, 83.6% of proteins were removed with an EV recovery of about 65% (Cho et al. 2016). In another study, a low-voltage indirect dielectric device comprised of an array of borosilicate micropipettes was capable of selective entrapment of exosomes from cell culture media, plasma, serum, and saliva, via their unique dielectric properties. By applying 10 V cm^{-1} direct current, the small conical pore of the pipette induced a non-uniform electric field, which in turn created a dielectrophoretic force near the pipette tip. This force was balanced by electroosmosis and electrophoresis, producing an entrapment area. The exosomes were isolated in only 20 minutes from 200 µL samples (Shi et al. 2019).

Paper-based microfluidic systems are also promising for enrichment and isolation of EVs. Recently, an origami design consisting of accordion-like multi-folded layers was integrated with ion concentration polarization, and an electric current was applied. This electrokinetic method enabled the preconcentration of EVs through separation of microvesicles and exosomes from proteins in specific layers of the device (Lee et al. 2020).

More recently, the electrophoretic approach has been combined with immunoaffinity methods to enhance the efficiency of isolation. Besides isolation, these microfluidic devices are also able

to concentrate and analyse (Guo et al. 2020; Guzman and Guzman 2020). For example, an antibody-functionalized multiplex paper-based technology was developed for separation of exosomes from large EVs, followed by electrokinetic concentration of exosomes. The analysis can also be based on surface proteins since they influence the electrophoretic mobility of exosomes. A serum-spiked mixture with exosomes from prostate cancer cells or a healthy control, labelled with fluorescent dyes, was used to evaluate the efficiency of the system. The detection results showed to be 30-fold more effective in comparison to enzyme-linked immunosorbent assays (ELISA) (Guo et al. 2020).

2.2.3. Nanowire trapping

Inorganic nanowires present mechanical stability, high surface-to-volume ratio, and can be embedded in microchannels. Due to its biocompatibility, ZnO nanowires are commonly used in microfluidic devices, but other materials can also fulfil the task, such as silicon (Dong et al. 2019a; Wang et al. 2013) or PDMS (Yasui et al. 2017). In the case of Wang et al. (2013), ciliated micropillars consisting of porous silicon nanowires on the side walls of the micropillars were built for multi-scale filtration. Fluorescently labelled liposomes were used as model vesicles, and it was shown that the system preferentially trapped exosome-like liposomes: 83 nm liposomes had a recovery rate of 60%, whereas 120 nm liposomes showed only 15% (Wang et al. 2013).

Even though nanowire trapping is usually classified as a label-free separation technique, it can be combined with immunoaffinity for better results. For example, Chen et al. (2018) built a PDMS-based microfluidic device covered with a ZnO nanowire array functionalized with anti-CD63. The system provided a larger area for exosomes trapping and a size-exclusion effect. The detection and quantification of exosomes was then performed by a colorimetric approach (Chen et al. 2018) (Fig. 3). In another work, Suwatthanarak et al. (2021) used a ZnO nanowire array fabricated within the microfluidic device, but functionalized with the EWI-2 peptide, which binds to CD9. After isolation, exosomes could be released using a NaCl solution (Suwatthanarak et al. 2021).

2.2.4. **Deterministic Lateral Displacement (DLD)**

DLD is a size-based technique able to sort particles from 100 nm to 30 μm. It uses pillar arrays that generate a fluid bifurcation and streamlines between gaps. Therefore, particle flow is determined by fluidic forces and the obstacle effect created by the pillars. When the particle radius is smaller than the gaps between pillars, it follows the initial streamline; in the case of being larger, it is bumped to the pillar and laterally displaced to another streamline (Salafi et al. 2019). Biagioni et al. (2020) anticipated the performance of DLD with a theoretical model, considering different forces for particle motion: electrostatic force, hindrance and diffuse effects (Biagioni et al. 2020). Furthermore, so that DLD can work as an efficient method for EVs separation, pillar arrays need to translate into the nanoscale for high yield separation of particles with a diameter as small as 20 nm. For that, DLD arrays with gap sizes ranging between 25 nm and 235 nm were tested, showing that their length influences the efficiency of separation, according to the diameter of the vesicle. For example, DLD is only effective for particles with 20 nm of diameter if the gaps are smaller than 42 nm. However, more than 200 kPa of input pressure was required for the motion of the vesicles, which withdraws the aim of a passive separation, besides limiting its clinical application (Wunsch et al. 2016). Therefore, Hattori et al. (2019) combined the nanopillar chips with electroosmotic flow (by application of an electric field) to overcome the need of high pressure to transport the EVs through the nanopillars (Hattori et al. 2019).

Only a few works based on DLD for EVs separation can be found in the literature. One of them belongs to Santana et al. (2014), who obtained a microfluidic device able to recover microvesicles from a pancreatic adenocarcinoma cell line with an efficiency of 39%, and a purity of 98.5% (Santana et al. 2014). In the work of Smith et al. (2018), also a size-based EV separation device was constructed based on nanoscale DLD arrays on a single chip, capable of processing several samples at rates up to 900 μL per hour. The research team compared its efficiency with ultracentrifugation, size exclusion chromatography and other techniques, demonstrating that their device was faster and had a higher yield of EVs, which could reach values bigger than 50% for serum and urine samples (Smith et al. 2018).

2.2.5. Viscoelastic flow

Liu et al. (2017) took advantage of particle migration due to size-dependent elastic lift forces in a viscoelastic medium. In comparison to microfluidics resorting to acoustics, electrophoretic or magnetic techniques, viscoelastic manipulation is not only a label-free technique, but also dismisses external applied fields. The microfluidic device had a middle outlet and two-sided outlets. The sample was introduced into the microchannel and mixed with poly(oxyethylene) solution to increase fluid viscoelasticity. Thus, the nanoparticles were laterally driven toward the microchannel centreline with different speeds, depending on the size, and controlled by the elastic lift forces. This way, large nanoparticles migrated faster to the centreline and were collected in the middle outlet, whereas small nanoparticles were collected at the other outlets. Thus, it was possible to separate exosomes from other larger EVs of cell culture medium or serum, with a recovery percentage above 80% (Liu et al. 2017) (Fig. 4).

Liu et al. (2019) designed a microfluidic system for size-selective separation of exosomes, microvesicles and apoptotic bodies, which used a viscoelastic fluid and a Newtonian sheath fluid (without elasticity). This caused the appearance of three forces: the elastic lift force, the inertial lift force, and the viscous drag force. The competition between these forces depends on the size of the particles, thus their migration pattern from the initial position to the sidewalls of the microfluidic device varied in a size-dependent manner. The isolation of EVs ranging from 100 nm to 2 µm took only 30 minutes (Liu et al. 2019). However, using inertial forces in Newtonian fluids is still difficult to implement in nanoscale systems because Brownian motion of the particles increases with the decrease of their size (Asghari et al. 2020).

To date, viscoelastic microfluid devices are underdeveloped for nanoparticles manipulation due to limitations of diffusivity of nanoparticles and channel length. To overcome such issues, Asghari et al. (2020) developed an oscillatory viscoelastic device. The microfluidic platform included a pressure-driven microfluidic chip coupled with an electronic circuit to generate oscillatory flow. Besides oscillatory flows being able to eliminate the need for long microchannels, the combination with viscoelastic flow helps overcome Brownian motion. This

way, it was possible to separate particles and biological species with diameters from only 20 nm to a few micrometres (Asghari et al. 2020).

3. Biosensing EVs

Detection of EVs has been gaining interest due to their link to health status, with great prospects for disease early diagnosis and therapeutic approaches (Bu et al. 2019). The aim is to translate their importance in cell communication into measurable signals in point-of-care (POC) setups. EVs as a new prognostic biomarker have listed advantages over other blood-based biomarkers, such as circulating tumour cells (CTC), circulating tumour DNA (ctDNA) and microRNAs. First, EVs are found in higher concentrations with respect to CTC, ctDNA and microRNAs in biofluids (Boriachek et al. 2018). Second, they contain a set of molecules specific to the origin cells, which get protected from the enzymatic action inside the EVs or in the lipid bilayer (Bu et al. 2019).

POC technologies are meant to be simple and avoid pre-processing of samples, so that any health professional can efficiently manipulate them. Such POC demand can be fulfilled by biosensors, whose implementation in our everyday lives is progressing fast due to their versatility and easy application. A biosensor is a sensing device that converts the reaction originated from the biorecognition of the analyte into a measurable signal, which includes electrochemical, optical, thermometric, magnetic or piezoelectric approaches (Asal et al. 2019; Kawamura and Miyata 2016). Biosensors bring great advantages over conventional techniques such as ELISA or polymerase chain reaction (PCR), due to simplicity, possibility of miniaturization, automation, fast and sensitive analysis, thus deploying cost-efficient designs, amenable to functionalization and incorporation of nanomaterials (Pirzada and Altintas 2019).

It should be noted that recent literature demonstrates a significant trend towards adaptation of biosensors to a lab-on-a-chip format, thus combining the precision of the original methods with very low sample volumes and potentially much lower operation costs. Furthermore, the progress

14

of micro and nanotechnologies allows the use of lab-on-a-chip formats in standard medicine, which opens new possibilities in EVs research (Chiriaco et al. 2018; Huang et al. 2020a).

3.1. Optical biosensors

3.1.1. Luminescence

Among the optical methods, fluorescence is a sensitive and versatile technique for detection of EVs with many sensor designs (Table 1). In the presence of a fluorescent molecule and a quencher, the system can be used to create a fluorescence "turn-on" (Li et al. 2020; Tayebi et al. 2019; Zhu et al. 2021) or a "turn-off" (Mori et al. 2019) signal. For example, a fluorometric biosensor was developed to detect exosomes derived from MCF-7 breast cancer cells. The detection method was based on immobilizing fluorescently labelled anti-CD63 on the surface of molybdenum disulphide-multiwall carbon nanotubes (MoS_2-CNT), which in turn acted as a fluorescence quenching material. When the exosomes bound to the anti-CD63 antibodies, there was a recovery of the fluorescence and the intensity increased with increasing concentration of exosomes (Tayebi et al. 2019) (Fig. 5). Li et al. (2020) also used a "turn-on" approach in the presence of the target exosomes. Graphene oxide (GO) was adopted as a quencher to the fluorescence signal of the positively-charged tertiary amine-containing tetraphenylethene (TPE-TA). The functioning principle of the system was the following: the TPE-TAs bound to aptamers targeting the exosomes surface protein prostate-specific membrane antigen (PSA), and that complex was absorbed in the GO system, thus the fluorescence signal was turned off. The targeted exosomes had higher binding affinity to the aptamers than GO, which led to the detachment of the complexes from the GO surface. In consequence, the fluorescent signal was turned on. Moreover, since numerous TPE-TAs could bind to a single aptamer, the fluorescence signal was amplified without enzymatic assistance (Li et al. 2020). A new technique based on molecularly imprinted polymers for fluorescence sensing of exosomes relied on the "turn-off" approach, which means that the fluorescent molecules are quenched when the target is present. The authors created post-imprinting in-cavity specific modifications, by introducing fluorescent markers and

15

immobilizing the antibody anti-CD9. The imprinted polymer cavities containing the fluorescent markers enabled detection of intact exosomes since fluorescence intensity was quenched with increasing concentration of exosomes (Mori et al. 2019). The imprinted nanocavities can be formed with template exosomes secreted from specific cell lines (Mori et al. 2019), or with functionalized nanoparticles (Takeuchi et al. 2020).

Other approaches were also used, as it is the case of the catalysis of tyramine by horseradish peroxidase (HRP), in presence of hydrogen peroxide, and the target exosomes. This reaction led to the production of a dimer and a fluorescence signal (Chen et al. 2020a). Dehghani et al. (2021) made the translation of an automated fluorescence technique originally developed for the characterization and quantification of viruses (Virus Counter 3100, Sartorius) to the quantification and profiling of EVs. The system works by emitting a laser light and capturing the emitted fluorescence from EVs previously labelled with fluorophores. Proof of concept was performed with polystyrene nanoparticles, showing that the performance of the analysis in the virus counter surpasses the conventional technique Nanoparticle Tracking Analysis (NTA) because it did not mask small particles (Dehghani et al. 2021).

For amplification of the fluorescence signal, which leads to increased sensitivity, several strategies have been pursued, such as the integration of nanoparticles. For example, nanovesicles were captured by cholesterol-modified magnetic beads and exosomes were further identified by copper oxide nanoparticles (CuONPs), modified with CD63 aptamers, and forming a sandwich complex. After targeting the exosomes, CuONPs in the complex were dissolved by acidolysis. In this way, the copper oxide turned into copper (II) ions, which in turn were reduced by sodium ascorbate to form fluorescent copper nanoparticles (CuNPs) in the presence of poly(thymine). Therefore, the fluorescence intensity was proportional to the concentration of exosomes. This method allowed a limit of detection (LOD) of 4.8×10^4 particles μL^{-1} in human serum (He et al. 2018). The sensitivity of fluorescence-based techniques can also be increased through the integration of other type of nanomaterials in sensor designs, like magnetic nanobeads (Kabe et al. 2019), plasmonic metallic nanostructures (Min et al. 2020), or quantum dots (Wu et al. 2021) (Table 1).

Signal enhancement using rolling circle amplification (RCA) has been also pursued (Huang et al. 2018; Huang et al. 2020b). As an example, Huang et al. (2018) utilized anti-CD63 modified magnetic beads conjugates to isolate leukaemia-derived exosomes, which were also recognized by surface expressed nucleolin using a DNA primer containing a nucleolin-recognition aptamer. The DNA primer initiated the RCA reaction to generate many repeat sequences to hybridize with a conjugate of gold nanoparticles (AuNPs). These AuNPs were functionalized with the antisense sequence of the DNA primer connected to a fluorescent dye (quenched at this state). Finally, a nicking endonuclease was introduced in the system to release the fluorescent dye, which changed from the quenching to the emission state. Furthermore, the conjugates were released and could be recycled. The described platform enabled reaching a LOD of 1×10^2 particles μL^{-1} (Huang et al. 2018) (Fig. 6).

An alternative amplification strategy was presented by Wang et al. (2020), using a molecular nanomachine with automatic walking, and a spider-looking configuration. It was denominated as 3D multipedal DNA walker. The aim of this work was to detect exosomes from lymphoblastic leukaemia, which present the protein tyrosine kinase 7 (PTK7) in abundance. The construction of the 3D multipedal DNA walker involved the use of a PTK7-targeting aptamer tailored at the 5' end of a catalyst by a poly-T linker, which was partially hybridized with anchored DNA conjugated on Sepharose beads. In the presence of the target exosomes, the aptamer recognition and binding to over-expressed PTK7 receptors led to their release from the beads and a 3D DNA structure like a spider was formed. The walker movement was then obtained by catalytic recycling. In this system, the DNA legs of the multipedal walker hybridized to the toehold of hairpin DNA1 (H1) conjugated on the surface of Sepharose beads opening the H1 structure. Then, the exposed DNA area of H1 could interact with another added DNA-hairpin fluorescently labelled (H2), which resulted in the migration of the DNA walker to an adjacent hairpin, triggering a new cycle. This approach led to a LOD of only 1 particle μL^{-1} (Wang et al. 2020b).

Recently, Zhao et al. (2020) published a method based on the amplification of exosomes recognition signal by the CRISPR-associated protein Cas12a system. To capture the exosomes, a CD63 aptamer partially blocked with complementary DNA strands (blocker) was used. The

interaction of exosomes with the CD63 aptamer caused a conformational change that released the blocker. The blocker was then recognized by the CRISPR/Cas12a system, which in turn triggered the cleavage of a fluorescent reporter probe labelled with Cy3 and Black Hole Quencher at both terminals, releasing the Cy3 fluorochrome. The fluorescent signal greatly amplified by this system was indicative of the captured exosomes, enabling a detection range of 10^3 to 10^7 particles μL^{-1} (Zhao et al. 2020).

Microfluidic devices with fluorescence detection have been gaining advantage as they enable isolation and concentration of EVs, single-EV sensitivity, quantification, and characterization, as well as automation in the same apparatus (Cheung et al. 2018; He et al. 2014; Ishihara et al. 2017; Zhao et al. 2016). Zhang et al. (2016) presented an ultrasensitive detection method for exosomes based on a microfluidic platform with GO and polydopamine nanointerface. This nanostructured interface designed to enhance the capture efficiency of exosomes enabled an ultrasensitive ELISA assay with enzymatic fluorescence signal amplification upon detection of exosomes from colon cancer cells, reaching a LOD of 50 exosomes μL^{-1} (Zhang et al. 2016). Zhang et al. (2020) developed a 3D nanoengineered chip through colloidal inkjet printing, for EV identification and monitoring of tumour growth. Metalloproteinases (MMPs) are known to be carried by EVs derived from tumour microenvironments. In particular, the MMP14 has major importance for the remodelling of extracellular matrix and activation of others MMPs. Thus, a peptide substrate labelled with a fluorophore and a quencher was added to the microfluidic device, which could be cleaved by the MMP14. When the EVs were present and cleavage occurred, the fluorescence signal appeared. Two ELISAs tests were also incorporated into the chip, to quantify the MMP14 content, and the EVs abundance by probing CD63 and CD9. The design of the microfluidic system allowed to conduct two samples at the same time, as well as two negative control assays. Clinical plasma from patients with ductal carcinoma or breast cancer was analysed with this microfluidic system, showing great accuracy (Zhang et al. 2020c).

Beyond detection with microfluidic systems, microarrays are powerful tools for the simultaneous analysis of several samples, being usually employed for screening antibodies or antigens, as well as to study protein interactions in less time-consuming assays. They allow highly

18

sensitive, cheap, and rapid throughputs, consuming only small sample volumes. Some studies have already shown the efficiency of microarrays for quantification and phenotyping of EVs. Those microarrays are usually based on choosing specific antibodies, peptides or aptamers targeting surface markers for profiling of EVs (Gori et al. 2020; Jin et al. 2018; Jorgensen et al. 2013; Liu et al. 2018a). ExoScreen is a fluorescence-based technique able to identify exosomes from blood without the need of purification steps. This system is composed of donor and acceptor beads: streptavidin-coated donor beads are used to capture an analyte-specific biotinylated antibody, while the acceptor beads are conjugated to the second antibody that recognizes an epitope of the analyte. When the donor beads are excited with a laser at 680 nm, singlet oxygen is released that excites the fluorescent signal in the acceptor beads at 615 nm. However, this is only possible if the beads are within 200 nm of the captured analyte, thus excluding larger EVs. The reliability of the test for profiling circulating exosomes was assessed by targeting two tetraspanin family proteins, CD9 and CD147, used as double confirmation for EVs derived from colorectal cancer (Yoshioka et al. 2014).

The sensitivity of luminescence-based techniques can also be increased through the integration of conductive materials, achieving a phenomenon denominated electrogenerated chemiluminescent (ECL), in which an electrochemical reaction leads to light emission (Zhang et al. 2020a; Zhang et al. 2019a; Zhang et al. 2019b). For instance, an electrode interface was modified with anti-CD63 aptamer, and AuNPs decorated with Ti_3C_2 MXenes also modified with the same aptamer were formed *in situ*, acting as ECL probes. When the exosomes were captured on the electrode, the MXenes linked to their surface and acted as a conductive support to AuNPs, improving their catalytic activity, and the detection was based on the ECL signal of luminol. This system enabled a LOD of 30 particles μL^{-1} for exosomes derived from cervical cancer cells (Zhang et al. 2020a).

3.1.2. Surface plasmon resonance (SPR)

Surface Plasmon resonance (SPR) is based on the excitation of electrons at the interface of a dielectric and conductive metal surface (usually silver or gold) with polarized light. SPR

biosensors are ideal for analysis of EVs due to their easy adaptability (Dobhal et al. 2020; Liao et al. 2020; Reiner et al. 2017a; Sina et al. 2016; Yang et al. 2020) (Table 1). An example of the versatility of SPR systems can be found in the approach of Im et al. (2014). Instead of total internal reflection, the system was adapted to measure the optical transmission through periodic nanoholes on a metal surface, and it was named nano-plasmonic exosome sensor. Each periodic array of nanoholes was functionalized with specific antibodies to detect surface proteins and those from exosome lysates. This study revealed a pattern in the expression of CD24 and EpCAM proteins, from exosomes isolated from ovarian cancer cells, also demonstrating a major improvement of the LOD regarding other techniques such as western blotting and ELISA (Im et al. 2014). Another example regards Qiu et al. (2019), whose novelty of the work was using a TiN support material instead of gold or silver. TiN is a biocompatible material with plasmonic characteristics in the visible-to-near-infrared spectrum, with tunable electric conductivity and optical absorption. The results showed better sensitivity and selectivity for glioma-derived exosomes when compared to conventional gold SPR biosensors (Qiu et al. 2019) (Fig. 7). Chen et al. (2020b) amplified the SPR signal using DNA hydrogel functionalized AuNPs. The mass cumulative effect of the hydrogel and the localized SPR effect of the AuNPs enhanced the signal of prostate cancer-derived exosomes (Chen et al. 2020b). Yildizhan et al. (2021) used an in-house made fibre optic SPR platform and established a calibration curve for recombinant EVs (rEVs) with a well-characterized surface composition. To increase sensitivity, different combinations of EV-specific antibodies were tested. Moreover, complex matrices were also evaluated, such as cell culture medium with rEVs and EVs from different cell lines, as well as in diluted blood plasma (Yildizhan et al. 2021).

The SPR technique has already been adapted to microarrays, which dismiss enrichment or purification of the samples. For example, a work demonstrated the combination of SPR imaging with antibody microarrays specific for membrane proteins of EVs from tumour cell culture medium (Zhu et al. 2014). Many studies have also demonstrated the ability of SPR techniques to be applied to biological samples and distinguish subpopulations of EVs (Fan et al. 2020; Picciolini et al. 2018; Rupert et al. 2016; Thakur et al. 2017).

3.1.3. Surface-enhanced Raman spectroscopy (SERS)

SERS is a technique for the enhancement of Raman scattering of analyte molecules that are adsorbed on/or near SERS-active surfaces, i.e., rough, or nanostructured metal surfaces, often relying on the classic use of gold or silver. It is a non-invasive technique for characterization and sensing, operating with small volumes and minimum sample preparation (Merdalimova et al. 2019).

Biosensors based on SERS can be label-free (Dong et al. 2020; Fraire et al. 2019; Jalali et al. 2021; Lee et al. 2015a; Rojalin et al. 2020; Sivashanmugan et al. 2017; Stremersch et al. 2016; Tirinato et al. 2012; Yan et al. 2019) or depend on labelling (Hou et al. 2020; Kwizera et al. 2018; Lee et al. 2017; Li et al. 2018; Ning et al. 2020; Tian et al. 2018; Wang et al. 2020c; Wang et al. 2020e; Wang et al. 2018b). The label-free approach allows reliable spectral fingerprint of the analyte and its identification in complex mixtures. Even though the label-free method is simpler, the efficiency of the sensor is surpassed by labelling in blood and serum samples, because it avoids signals from interfering molecules that are co-adsorbed (Merdalimova et al. 2019).

Regarding label-free SERS biosensors, Tirinato et al. (2012) used super-hydrophobic silicon micropillars coated with silver nanograins to distinguish exosomes derived from healthy and tumour colon cell lines, through the changes in SERS spectra. Since the super-hydrophobicity reduces the friction coefficient, this property is used to concentrate diluted samples in very small regions, and this increased density results in enhanced SERS signals (Tirinato et al. 2012). Lee et al. (2015) also utilized the label-free approach as a simpler and faster alternative to the conventional biochemical analysis of exosomes. The authors used nanobowl-structured plasmonic substrates to capture exosomes from the SKOV3 cell line. The surface of the SERS sensor was fabricated via soft lithography on PDMS, where a layer of silver was sputtered, thus creating the nanobowls. These structures enabled the capture and entrapment of the exosomes, besides allowing discrimination between intact and ruptured exosomes (Lee et al. 2015a). Following a similar approach, in the work of Sivashanmugan et al. (2017), exosomes were detected at concentrations of 10^4-10^5 lower than normal blood samples. For that, the SERS

substrate combined silver nanocubes on a surface with gold nanorods. This combination also enabled the distinction between exosomes released by normal and cancerous lung cells (Sivashanmugan et al. 2017). An innovative work was designed by Fraire et al. (2019), which attached AuNPs directly to the EVs membrane through electrostatic forces, followed by overgrowing them with a silver layer *in situ*. This improved the signal-to-noise quality and resulted in a specificity and sensitivity higher than 90% for the discrimination between red blood cells and EVs from melanoma cells (Fraire et al. 2019). More recently, Dong et al. (2020) created a macroporous inverse opal (MIO) structure, assembled to mimic natural beehives, to capture and analyze the exosomes extracted from plasma of cancer patients. For that, an opal of PS nanoparticles was infiltrated with titanium oxide (TiO_2), and the nanoparticles were subsequently removed to create the MIO. The TiO_2 MIO structure was then coated with Au. The pores of the MIO act as a trap for light, enhancing the SERS signal (Dong et al. 2020) (Fig. 8).

One example of the labelling approach for SERS assays regards the work of Kwizera et al. (2018). A 3D printing array technology was used to create an antibody matrix to capture exosomes on gold-covered slides. Then, the exosomes captured through the target-specific antibodies were labelled using SERS nanotags composed of gold nanorods and a non-fluorescent organic dye (QSY21) as Raman reporter. In this study, human epidermal growth factor receptor 2 (HER-2) and EpCAM were identified on exosomes from patients with breast cancer in plasma samples, revealing its feasibility for molecular profiling (Kwizera et al. 2018). Another work carried out by Tian et al. (2018) demonstrated the immunomagnetic capture of exosomes, followed by the formation of sandwich-type complexes between the SERS nanoprobes, exosomes and magnetic beads. The magnetic nanobeads were modified with antibodies to recognize CD9 proteins on the exosome membrane. The nanoprobes were produced with nanostar shapes and modified with bivalent cholesterol-labelled DNA chains that bind to the exosome membrane through hydrophobic interaction. The establishment of such complexes enabled the magnetic enrichment of SERS nanoprobes, only possible in the presence of targeted exosomes. Thus, SERS signal is only detectable in the presence of exosomes, and this device presented a LOD as low as 27 particles μL^{-1} (Tian et al. 2018) (Table 1). Ning et al. (2020) used bimetallic SERS-active

nanotags for the simultaneous detection of different cancer-related exosomes. There were two types of probes in the system: the capture probes, constituted by magnetic beads modified with aptamers targeting exosomes; and the detection nanotags, made by a core of gold and two shells of silver, decorated with DNA sequences complementary to the aptamers. Therefore, in the absence of exosomes, the detection probes hybridized with the capture probes. When exosomes were present, they interacted with the capture probe, releasing the SERS nanotags. Therefore, the SERS signal decreased in the presence of the biomarker. Distinct exosomes were detected, based on different kinds of SERS nanotags, via different Raman reporter molecules or linker DNAs (Ning et al. 2020).

The SERS-based EVs detection was already adapted to chips, able to monitor changes of the EV profile of patients undergoing melanoma-related therapies. The chip incorporated a multiplex SERS nanotag system, without the need of EV enrichment from plasma samples. The nanotags were composed of AuNPs bound to Raman reporters in conjunction with tumour-specific antibodies. This system allowed to detect different EVs phenotypes from eight melanoma patients, which gathers great potential at studying treatment responses, such as the development of drug resistance (Wang et al. 2020c).

3.1.4. Colorimetric

Colorimetric strategies developed to detect EVs usually resort to particles aggregation when the bioanalyte is present (Jiang et al. 2017; Wang et al. 2021b) or through catalytic reactions (Chen et al. 2018; Wang et al. 2017b; Xia et al. 2020; Xia et al. 2017; Yang et al. 2019; Zeng et al. 2021; Zhang et al. 2020d; Zhang et al. 2021; Zhou et al. 2019a), both methods leading to a colour change. An example of the first approach is the work of Jiang et al. (2017), which developed a colorimetric sensor to detect exosomes based on aptamer/AuNPs complexes. A panel of aptamers was chosen to profile exosome surface proteins. This study showed that complexation of aptamers with AuNPs prevented aggregation of the particles, but in the presence of exosomes, the aptamers specifically bind to exosomes surface proteins rather than the non-specific, weak binding to the AuNPs. As the complex is broken, by displacing aptamers from AuNPs surface, it

23

leads to aggregation of the particles and colour change (Jiang et al. 2017). Regarding the second approach, Yang et al. (2019) used commercially available pH strip tests for a quantitative analysis of exosomes. Briefly, the study reports that exosomes were first captured by magnetic nanoparticles. Then, antibodies against CD63 conjugated to HRP catalyse the formation of a polydopamine film on exosomes surface, which in turn allows the binding of urease. By adding urea to the system, urease converts it into ammonia, increasing the pH value, which is noticeable in pH strips by colour change (Yang et al. 2019) (Fig. 9). Zhang et al. (2020) used a different strategy, resorting to exosome-triggered etching of gold nanobipyramid@MnO_2 nanostructures. In summary, CD63 aptamer and two sequences partially complementary to CD63 labelled with alkaline phosphatase (P-ALP) were linked to magnetic beads. When exosomes are present, their binding to the CD63 aptamer is stronger than that of P-ALP, thus those sequences are released. Then, the L-ascorbic acid 2-phosphate present in the reaction system is dephosphorylated by P-ALP producing ascorbic acid, which, in turn, etches the MnO_2 nanosheets, leading to a morphological change of the nanoparticles. The morphological change leads to a difference of their refractive index, thus to a colour change. This method achieved a LOD of only 135 exosomes μL^{-1} (Zhang et al. 2020d). Xu et al. (2020) presented a different study adding dopamine and hydrogen peroxide solution to a complex of exosomes captured by CD63 specific aptamer conjugated to HRP. The colour intensity of the transformation of dopamine into dark polydopamine correlated well with the concentration of exosomes. The LOD obtained was 7.7 particles μL^{-1} (Xu et al. 2020) (Table 1).

Colorimetric approaches based on lateral flow immunochromatographic strips have also been developed. The strips showed successful at detecting exosomes from a human metastatic melanoma cell line, making use of antibodies against tetraspanins and AuNPs for the colorimetric response. However, the LOD was high comparing to previous literature, attaining 8.54×10^5 exosomes μL^{-1} (Oliveira-Rodriguez et al. 2016). Exosomes were also detected with immunochromatographic strips decorated with iron oxide nanoflowers coated with a carbon layer. The magnetic core allowed magnetic isolation, whereas the carbon coating held functional groups needed for bioconjugation. The LOD obtained was around 10^6 EVs μL^{-1} (Moyano et al. 2020).

24

There are also some works using colorimetric biosensors not only to determine EVs concentration, but also their purity (Maiolo et al. 2015; Zendrini et al. 2019). The principle is related to the ability of colloidal AuNPs to adsorb and cluster at the membrane of EVs, which does not occur when the samples contain single and aggregated protein contaminants. If the preparation of EVs is pure, the solution turns blue due to the aggregation of AuNPs at the membrane of EVs and stays red in the presence of protein contaminants as the first phenomenon is inhibited (Maiolo et al. 2015).

In addition, it is also truly important to have a strong optical signal with high sensitivity, since EVs are generally studied for an early detection of a certain disease, which implies that their concentration in biological samples is low. In the context of amplifying the detection of tumour-derived exosomes, a study used a proximity ligation assay, which involves DNA-assisted protein detection (Liu et al. 2018b). The proof-of-concept was applied to nasopharyngeal carcinoma samples that possess LMP1-positive and EGFR-positive EVs. Briefly, a pair of antibodies against LMP1 was coupled to DNA reporter sequences that hybridize when in close proximity after synchronous recognition of LMP1 on the exosomes. Then, exosomes are separated from the remaining sample using magnetic beads functionalized with antibodies against tetraspanins. Through recombinase polymerase amplification and transcription-mediated amplification, multiple copies of RNA transcripts from the DNA signal are formed, and then hybridize with the complementary sequence present on AuNPs. In this way, the nanoparticles aggregate, shifting the colour from red to blue. The determined LOD achieved the lowest value observed so far in colorimetric assays of 0.1 particles μL^{-1} (Liu et al. 2018b) (Fig. 10).

3.1.5. Photonic structures

In the last years, even though in less number, some studies for detection and quantification of EVs uses photonic crystals (PCs). Wang et al. (2018) constructed a photonic biosensor for targeting host exosomes, distinguishing them from the ones derived from parasitic nematodes. The photonic part consisted of a one-dimensional grating substrate, coated with a high-refractive index thin film (acting as a light confinement layer for resonance modes), and functionalized with

25

anti-CD63. Exosomes from the parasites do not present CD63 at the membrane surface, therefore the capture of host exosomes is specific, increasing the refractive index of the biosensor, which results in a shift in the wavelength of the reflected light (Wang et al. 2018a). Recently, the same research group used a similar device, but explored the transmission spectrum of the PC substrate to differentiate between different types of macrophage-derived EVs. Since their recognition caused a distinguishable wavelength shift, the detection process was based on the spectral signature of each EV (Wang et al. 2021c).

The design of PC structures has also been explored in combination with other signal readings. In the work presented by Zhu et al. (2018), a 3D plasmonic PC with point-defect cavities was constructed, which showed the hybrid coupling of plasmonic and PC modes, increasing the electromagnetic field intensity and sensitivity (Zhu et al. 2018). Another sensor with high sensitivity was developed by Dong et al. (2019), which built a chip with a double-filtration unit and a sensor based on PC nanostructures named ExoID-Chip. It integrated a nanofiltration membrane to enrich EVs ranging 20-200 nm based on size-exclusion. Then, the isolated EVs were combined with excessive aptamers targeting CD63 and quantified by a competitive immunoassay. Therefore, the aptamers in excess were detected on the PC layer that had immobilized CD63 and a fluorescence labelling reaction occurred, which used the PC as an enhancement factor of the fluorescent signal, allowing a LOD of 8.9 EVs μL^{-1} (Dong et al. 2019b) (Table 1). Zhang et al. (2020) detected exosomes from pancreatic cancer cells using quantum dots functionalized with antibodies targeting the glypican-1 membrane-anchored protein of exosomes. The PCs worked as a signal amplification system (Zhang et al. 2020b).

3.2. Electrochemical biosensors

In electrochemical biosensors, the recognition chemical reaction produces or consumes ions or electrons, which leads to measurable electrical variations in current, potential, or impedance. It is the most widespread approach, due to its typical high sensitivity, ability of inclusion in portable devices and cheap fabrication (Li et al. 2017; Monošík et al. 2012). For example, the detection of released EVs from breast cancer cells upon induced hypoxia or normoxia conditions,

used gold electrodes functionalized with antibodies against CD81 to capture the EVs. The detection was followed by electrochemical impedance spectroscopy (EIS) and differential pulse voltammetry (DPV), achieving LODs of 0.077 EVs μL^{-1} and 0.379 EVs μL^{-1}, respectively (Kilic et al. 2018).

A sandwich-type electrochemical immunoassay was reported by Doldán et al. (2016), and the sensor could detect 200 exosomes μL^{-1} of serum samples with volumes as low as 1.5 μL (Table 2). The gold surface on the working electrode was modified with an anti-CD9 antibody to specifically capture exosomes. Then, mouse anti-human CD9 antibodies, different from those anchored on the gold surface, were added to recognize the many exposed CD9 molecules on the surface of exosomes, thus amplifying the signal. Finally, mouse anti-IgG antibodies conjugated to HRP were able to recognize mouse anti-CD9 and bind to the system. Detection was achieved by electrochemical reduction of HRP-oxidized 3,3',5,5'-tetramethylbenzidine (TMB), which leads to differences in current, directly dependent on the exosomes concentration (Doldan et al. 2016). Also, in a sandwich-based assay, another electrochemical method was reported to quantify exosomes from breast cancer cells. Exosome capture was performed using anti-CD9 antibodies immobilized on the surface of a screen-printed carbon electrode. The detection step was performed by using antibodies against HER-2, generating current differences according to the number of recognized exosomes. To monitor the current generated in each step, DPV was used in the presence of the redox system $[Fe(CN)_6]^{3-/4-}$ (Yadav et al. 2017). More recently, a LOD as low as 5 EVs μL^{-1} was achieved using a sandwich immunoassay implemented on a lab-on-a-chip design. It combined an enzymatic reaction with a redox cycling on nanointerdigitated electrodes (Mathew et al. 2020).

Another technique for the detection of EVs resorts to nanoparticle-labelling, which depends on functionalized metal nanoparticles to bind to the target, and a gold electrode to sense the introduced differences on impedance, current or voltage. In a work developed to investigate such application, gold electrodes were modified with thiolated anti-EpCAM aptamers to bind to the EVs. Silver nanoparticles (AgNPs) and copper nanoparticles (CuNPs) were used as probes, since their oxidation potentials fall in the potential window of the gold electrodes and are well separated

27

from each other, enabling multiplex exosomal protein detection. AgNPs were functionalized with anti-EpCAM, and CuNPs were functionalized with anti-PSA, which is specific to prostate cancer. Linear sweep voltammetry was then applied for the oxidation of the metal nanoparticles, leading to an electrochemical peak related to the presence and the amount of each surface marker. This study not only showed a new technique for EVs detection, but also a platform for different protein marker detection (Zhou et al. 2016b) (Fig. 11). In a recent work develop by Wang et al. (2020d), covalent organic frameworks (COFs)-based nanoprobes were prepared by functionalization with HRP and with AuNPs bound to a linker that recognized amino acid residues of the exosomes surface. In the presence of exosomes, the HRP catalysed the oxidation of TMB in the presence of hydrogen peroxide creating an electrochemical signal. This technique was able to achieve a LOD of 160 particles μL^{-1} (Wang et al. 2020d) (Table 2).

Microfluidic electrochemical devices were also already developed for the purpose of detecting EVs. For example, Zhou et al. (2016) developed an effective and simple electrochemical biosensor for exosomes using the specific aptamer for CD63. The aptamers for CD63 were immobilized on the surface of gold electrodes and then incorporated into a microfluidic system. Antisense strands pre-labelled with redox probes were hybridized with the aptamers. In the presence of exosomes, and due to their interaction with the aptamers, there is a displacement of the probing strands and the electrochemical signal decreases (Zhou et al. 2016a). Wang et al. (2017) developed a portable electrochemical device, which used a DNA nanotetrahedron structure (NTH) for assisting the aptamer to detect and capture exosomes from hepatocarcinoma cells. Aptamer-containing NTHs were immobilized onto the gold electrodes, showing 100-fold higher sensitivity than when the biosensor was only based on the single-stranded aptamer (Wang et al. 2017a) (Fig. 12). In another work, a detachable microfluidic device was implemented with an electrochemical aptasensor. Whereas the aptasensor is obtained through the electrodeposition of gold nanostructures and the immobilization of EpCAM as the recognition element, the microfluidic device is a type of vortex used to enhance the impact between exosomes and the sensing surface. Removing this microfluidic component allows to subsequently harvest the

exosomes for downstream analysis. The device accomplished a LOD of 17 particles μL^{-1} (Kashefi-Kheyrabadi et al. 2020).

Moreover, self-powered electrochemical biosensors raise much interest because they do not need an external power source, thus miniaturization is easily achieved. For example, Gu et al. (2021) created a biofuel cell for the detection of exosomes. For that, glucose dehydrogenase within a metal-organic framework (MOF) was used at the anode, improving its stability. The cathode was modified with CD63 antibodies for the detection and capture of exosomes. When exosomes were present, MOFs loaded with electroactive molecules ($K_3[Fe(CN)_6]$) were applied, acting as receptors of the anode electrons derived from the oxidation of glucose. Under such conditions, an electrical current got formed, and a LOD of 0.3 exosomes μL^{-1} was obtained (Gu et al. 2021).

Nevertheless, the differentiation between cancer-derived exosomes and normal exosomes remains one of the major challenges together with signal amplification to achieve lower LODs, aiming the applicability of the developed biosensors in the clinic. Huang et al. (2019) addressed these requirements for gastric cancer detection. For that, a gold substrate was modified with anti-CD63, and a specific aptamer to gastric cancer-derived exosomes was added to the detection system. The aptamer was linked to a primer sequence complementary to a G-quadruplex circular template. RCA is triggered only in the presence of the target exosomes, producing several G-quadruplex units. Then, this HRP mimicking DNAzyme catalyses the reduction of hydrogen peroxide, thus creating an electric current. This sensor showed a LOD of 0.954 exosomes μL^{-1} (Huang et al. 2019). More recently, in the work of Wang et al. (2021), breast cancer-derived exosomes signal was amplified by using a multidirectional hybridization chain reaction. The gold electrode surface was functionalized with EpCAM to capture the exosomes. Then, cholesterol-modified H shape-like DNA unit 1 (cH1) was added to anchor to the exosome surface, and a second biotin-modified H shape-like DNA unit (H2) allowed to create a DNA structure. The DNA structure recruits a large quantity of streptavidin-HRP, due to interaction with biotin. The HRP catalyses the reaction between TMB and hydrogen peroxide, generating not only an electric current, but also a colour change of the solution. However, the LOD of 285 exosomes μL^{-1} stands

29

higher than in other explored electrochemical approaches (Table 2). Nevertheless, the sensor was capable of distinguish between cancerous and non-cancerous exosomes from culture cells and serum samples (Wang et al. 2021a).

Magneto-electrochemical sensors for analysis of EVs appeared recently, combining magnetic selection and electrochemical detection (Dong et al. 2018; Jeong et al. 2016; Lima Moura et al. 2020; Park et al. 2017; Xu et al. 2018). For example, Dong et al. (2018) used magnetic beads conjugated to aptamers targeting PSA to capture cancer exosomes, but their detection was indirectly based on measuring nucleic acids. Therefore, the PSA aptamers were hybridized with messenger DNAs (mDNAs), which were released when the exosomes were recognized. After magnetic separation, the concentration of released mDNAs was assessed by an electrochemical sensor based on cyclic enzymatic amplification (Dong et al. 2018). The work of Xu et al. (2018) targeted tumour-derived exosomes in serum by creating a two-stage microfluidic platform. The first stage corresponds to isolation by magnetic enrichment. Thus, Y-shaped micropillars were patterned for anisotropic flow of the sample, to increase the opportunities of linkage between exosomes and magnetic beads modified with phosphatidylserine-Tim4 protein. The second stage consisted of an aptasensor on ITO electrode, based on a probe containing an aptamer for CD63 recognition and a mimicking DNAzyme sequence. When exosomes were present, the single-stranded DNA hairpin sequence was opened, thus forming a G-quadruplex that combined with hemin acted as NADH oxidase and HRP-mimicking DNAzyme simultaneously, leading to the enhancement of the electrochemical signal (Xu et al. 2018) (Fig. 13).

3.3. Magnetic biosensors

As previously mentioned, magnetic approaches are usually used for specific separation and enrichment, being usually coupled with optical (Chen et al. 2020a; Chen et al. 2019; Moyano et al. 2020) or electrochemical techniques for the actual analysis and detection of EVs (Dong et al. 2018; Jeong et al. 2016; Lima Moura et al. 2020; Park et al. 2017; Xu et al. 2018). However, there are a few reports of microfluidic devices that depend only on magnetic properties for EVs detection. It is the case of the work reported by Shao et al. (2012), whose device was able to

profile blood-circulating microvesicles from glioblastoma patients. The blood was introduced into a microfluidic chip with magnetic nanoparticles, functionalized with anti-CD63 antibody, for specific EV labelling and isolation, followed by detection with a micro nuclear magnetic resonance system (Shao et al. 2012). Magnetoresistive sensors have been recently adapted to biological contexts, including the sensing of EVs, previously labelled with functionalized magnetic nanoparticles. These platforms allow fast quantification, without using large sample volumes, while enabling a pre-concentration due to the use of magnetic nanoparticles, which increases their sensitivity to the target (Cherré et al. 2017). For example, Cherré et al. (2017) developed a magnetoresistive biosensor chip capable of detecting 10^5 microvesicles μL^{-1} in less than an hour, a value that is within the physiological concentration range (Cherré et al. 2017) (Table 2). Wang et al. (2020) made use of the same technique not only to detect EVs, but also to profile the glycans at their surface. This was possible due to the use of functionalized magnetic nanoparticles and addition of specific lectins, which transduced specific EV-bound glycans measured in real time using an on-chip giant magnetoresistance (GMR) sensor (Wang et al. 2020g) (Fig. 14).

A recent work developed by Zhu et al. (2020) presented an ultrasensitive GMR biosensor based on molybdenum disulphide-iron oxide (MoS_2–Fe_3O_4) nanostructures as magnetic probes. The probes were modified with aptamers specific to cancer cell-derived exosomes. Each MoS_2 structure could collect several Fe_3O_4 nanoparticles, which increased the magnetic probes density, thus amplifying the target signal. The biosensor presented a LOD of 100 exosomes (Zhu et al. 2020).

3.4. Piezoelectric biosensors

Acoustic techniques depend on shifts of the frequency of an oscillating sensor due to alterations of the medium where the acoustic waves propagate. The oscillating sensor surface can be modified with specific capture probes, thus only responding to the adsorption/desorption of the target (Romanszki et al. 2020). In the work of Wang et al. (2020), the signal amplification

31

was attained with AuNPs. Briefly, a SAW sensor was functionalized with anti-CD63, which linked to the exosomes. Then, biotin conjugated EpCAM antibodies were added to the system, as well as streptavidin modified AuNPs. This way, a biotin-streptavidin interaction was obtained, and the AuNPs were attached to the target exosomes already recognized by the sensor. The AuNPs increased the acoustic waves phase shift, amplifying the recognition signal. It showed a LOD of 1.1 particles μL^{-1} from hepatic carcinoma cells. Moreover, the biosensor also showed to be successful at analysing blood samples of healthy and cancer patients (Wang et al. 2020a) (Fig. 15).

Another work used a quartz crystal microbalance with dissipation monitoring (QCM-D) to detect exosomes. The QCM was functionalized with antibodies against CD63, creating a direct immunoassay. The system showed detection of clinically relevant concentration of exosomes in spiked human serum, presenting a LOD of 2.9×10^5 or 1.4×10^5 exosomes μL^{-1} for frequency or dissipation responses, respectively (Suthar et al. 2020) (Table 2).

4. Conclusion and Future Perspectives

The importance of cell-to-cell transport of biomolecules in health and disease makes the research field of EVs one of the most fruitful. EVs are mediators of intercellular communication over near and far distances and are involved in a wide range of physiological processes, immune responses, disease progression, among many other biological functions. Great progress has been made in understanding the biogenesis, composition, trafficking of biomolecules, and function of EVs. Therefore, the study of EVs has increased in complexity and diversity, i.e., in various biofluids, from different biological sources (including interspecies communication), and for biotechnological and therapeutic approaches.

Along with the proliferation of studies on EVs, there has been a recognized effort and necessity in defining experimental requirements and standardization of procedures when isolating, identifying, and characterizing EVs, in terms of both content and function. According to the position statements from ISEV, MISEV2014 guidelines (Lotvall et al. 2014), updated in

MISEV2018 (Thery et al. 2018), researchers must report all technical details concerning EVs studies. This is crucial for reproducibility, and to meet purity requirements, so that information about particle number counts, biomarker analysis and functional activity gets reliable. However, at the moment, literature regarding EVs isolation protocols is still lacking uniformization. Moreover, classical techniques for isolation and characterization fail at maintaining EVs intact, besides showing low purity yields after time-consuming processes, and entailing high costs. The parallel ongoing technological advance on microfluidic devices is expected to contribute to improve the experimental load of isolating specific subpopulations of EVs, in a good yield and purity. Microfluidics have the advantage of being miniaturized, low cost, simple, and preserve EVs morphology. The pursuit in complying with specific guidelines and improve the microfluidic devices will certainly enhance the reliability and reproducibility of the research in this field.

Therefore, the next step leading to the clinical applicability of EVs as disease biomarkers is the improvement and simplification of their detection. The reviewed biosensors are cost- and time-effective and allow the investigation of low sample volumes with minimal amounts of EVs of interest. Even though many studies found in the literature still divide isolation and detection steps, the newest sensing layouts can have an extremely low LOD, while integrating multiple stages of isolation and characterization in the same device.

In comparison with the current standard methods, which most of the times require the use of successive different approaches, better and faster enrichment is expected from miniaturized sensors. Research is also aiming to get beyond bulk analysis, especially resorting to electrochemical and optical approaches, which both showed to be promising at single-vesicle level analysis. Nevertheless, the need for signal amplification is still hindering the simplicity of most of the developed systems. Furthermore, most studies evaluate the performance of biosensors using EVs derived from cell culture media. Since at clinical setup more complex samples are collected, such as blood, saliva, and urine, it is imperative to understand if parameters like sensitivity and selectivity are not hampered. The results obtained so far regarding the response of biosensors tested in real samples, including to distinguish EVs from healthy and diseased individuals, have been successful.

33

In conclusion, specific and sensitive functional readouts will continue providing new insights on the biochemical signatures of EVs and get the translation of POC devices to the clinic an upcoming reality. Furthermore, filling the gaps of current knowledge on how the enclosed information is generated, communicated, and implemented, will certainly leverage the therapeutic use of these vesicles as contributors to health status, from diseased conditions to aging.

5. Acknowledgements

References

Aharon, A., Spector, P., Ahmad, R.S., Horrany, N., Sabbach, A., Brenner, B., Aharon-Peretz, J., 2020. Extracellular Vesicles of Alzheimer's Disease Patients as a Biomarker for Disease Progression. Mol Neurobiol 57(10), 4156-4169.

Asal, M., Özen, Ö., Şahinler, M., Baysal, H.T., Polatoğlu, İ., 2019. An overview of biomolecules, immobilization methods and support materials of biosensors. Sensor Review 39(3), 377-386.

Asghari, M., Cao, X., Mateescu, B., van Leeuwen, D., Aslan, M.K., Stavrakis, S., deMello, A.J., 2020. Oscillatory Viscoelastic Microfluidics for Efficient Focusing and Separation of Nanoscale Species. ACS Nano 14(1), 422-433.

Baci, D., Chirivì, M., Pace, V., Maiullari, F., Milan, M., Rampin, A., Somma, P., Presutti, D., Garavelli, S., Bruno, A., Cannata, S., Lanzuolo, C., Gargioli, C., Rizzi, R., Bearzi, C., 2020. Extracellular Vesicles from Skeletal Muscle Cells Efficiently Promote Myogenesis in Induced Pluripotent Stem Cells. Cells 9(6), 1527.

Biagioni, V., Balestrieri, G., Adrover, A., Cerbelli, S., 2020. Combining Electrostatic, Hindrance and Diffusive Effects for Predicting Particle Transport and Separation Efficiency in Deterministic Lateral Displacement Microfluidic Devices. Biosensors (Basel) 10(9), 126.

Boriachek, K., Umer, M., Islam, M.N., Gopalan, V., Lam, A.K., Nguyen, N.T., Shiddiky, M.J.A., 2018. An amplification-free electrochemical detection of exosomal miRNA-21 in serum samples. Analyst 143(7), 1662-1669.

Broman, A., Lenshof, A., Evander, M., Happonen, L., Ku, A., Malmstrom, J., Laurell, T., 2021. Multinodal Acoustic Trapping Enables High Capacity and High Throughput Enrichment of Extracellular Vesicles and Microparticles in miRNA and MS Proteomics Studies. Anal Chem 93(8), 3929-3937.

Bu, H., He, D., He, X., Wang, K., 2019. Exosomes: Isolation, Analysis, and Applications in Cancer Detection and Therapy. Chembiochem 20(4), 451-461.

Bunggulawa, E.J., Wang, W., Yin, T., Wang, N., Durkan, C., Wang, Y., Wang, G., 2018. Recent advancements in the use of exosomes as drug delivery systems. J Nanobiotechnology 16(1), 81.

Chen, C., Skog, J., Hsu, C.H., Lessard, R.T., Balaj, L., Wurdinger, T., Carter, B.S., Breakefield, X.O., Toner, M., Irimia, D., 2010. Microfluidic isolation and transcriptome analysis of serum microvesicles. Lab Chip 10(4), 505-511.

Chen, H., Luo, D., Shang, B., Cao, J., Wei, J., Chen, Q., Chen, J., 2020a. Immunoassay-type biosensor based on magnetic nanoparticle capture and the fluorescence signal formed by horseradish peroxidase catalysis for tumor-related exosome determination. Microchim Acta 187(5), 282.

Chen, W., Li, J., Wei, X., Fan, Y., Qian, H., Li, S., Xiang, Y., Ding, S., 2020b. Surface plasmon resonance biosensor using hydrogel-AuNP supramolecular spheres for determination of prostate cancer-derived exosomes. Microchim Acta 187(11), 590.

Chen, Y.S., Ma, Y.D., Chen, C., Shiesh, S.C., Lee, G.B., 2019. An integrated microfluidic system for on-chip enrichment and quantification of circulating extracellular vesicles from whole blood. Lab Chip 19(19), 3305-3315.

Chen, Z., Cheng, S.B., Cao, P., Qiu, Q.F., Chen, Y., Xie, M., Xu, Y., Huang, W.H., 2018. Detection of exosomes by ZnO nanowires coated three-dimensional scaffold chip device. Biosens Bioelectron 122, 211-216.

Cherré, S., Fernandes, E., Germano, J., Dias, T., Cardoso, S., Piedade, M.S., Rozlosnik, N., Oliveira, M.I., Freitas, P.P., 2017. Rapid and specific detection of cell-derived microvesicles using a magnetoresistive biochip. The Analyst 142(6), 979-986.

Cheung, L.S., Sahloul, S., Orozaliev, A., Song, Y.A., 2018. Rapid Detection and Trapping of Extracellular Vesicles by Electrokinetic Concentration for Liquid Biopsy on Chip. Micromachines (Basel) 9(6), 306.

Chiriaco, M.S., Bianco, M., Nigro, A., Primiceri, E., Ferrara, F., Romano, A., Quattrini, A., Furlan, R., Arima, V., Maruccio, G., 2018. Lab-on-Chip for Exosomes and Microvesicles Detection and Characterization. Sensors (Basel) 18(10), 3175.

Cho, S., Jo, W., Heo, Y., Kang, J.Y., Kwak, R., Park, J., 2016. Isolation of extracellular vesicle from blood plasma using electrophoretic migration through porous membrane. Sensors and Actuators B: Chemical 233, 289-297.

Colombo, M., Raposo, G., Thery, C., 2014. Biogenesis, secretion, and intercellular interactions of exosomes and other extracellular vesicles. Annu Rev Cell Dev Biol 30, 255-289.

Coumans, F.A.W., Gool, E.L., Nieuwland, R., 2017. Bulk immunoassays for analysis of extracellular vesicles. Platelets 28(3), 242-248.

Davies, R.T., Kim, J., Jang, S.C., Choi, E.J., Gho, Y.S., Park, J., 2012. Microfluidic filtration system to isolate extracellular vesicles from blood. Lab Chip 12(24), 5202-5210.

Dehghani, M., Montange, R.K., Olszowy, M.W., Pollard, D., 2021. An Emerging Fluorescence-Based Technique for Quantification and Protein Profiling of Extracellular Vesicles. SLAS Technol 26(2), 189-199.

Dobhal, G., Datta, A., Ayupova, D., Teesdale-Spittle, P., Goreham, R.V., 2020. Isolation, characterisation and detection of breath-derived extracellular vesicles. Sci Rep 10(1), 17381.

Doldan, X., Fagundez, P., Cayota, A., Laiz, J., Tosar, J.P., 2016. Electrochemical Sandwich Immunosensor for Determination of Exosomes Based on Surface Marker-Mediated Signal Amplification. Anal Chem 88(21), 10466-10473.

Dong, H., Chen, H., Jiang, J., Zhang, H., Cai, C., Shen, Q., 2018. Highly Sensitive Electrochemical Detection of Tumor Exosomes Based on Aptamer Recognition-Induced Multi-DNA Release and Cyclic Enzymatic Amplification. Anal Chem 90(7), 4507-4513.

Dong, J., Zhang, R.Y., Sun, N., Smalley, M., Wu, Z., Zhou, A., Chou, S.J., Jan, Y.J., Yang, P., Bao, L., Qi, D., Tang, X., Tseng, P., Hua, Y., Xu, D., Kao, R., Meng, M., Zheng, X., Liu, Y., Vagner, T., Chai, X.,

Zhou, D., Li, M., Chiou, S.H., Zheng, G., Di Vizio, D., Agopian, V.G., Posadas, E., Jonas, S.J., Ju, S.P., Weiss, P.S., Zhao, M., Tseng, H.R., Zhu, Y., 2019a. Bio-Inspired NanoVilli Chips for Enhanced Capture of Tumor-Derived Extracellular Vesicles: Toward Non-Invasive Detection of Gene Alterations in Non-Small Cell Lung Cancer. ACS Appl Mater Interfaces 11(15), 13973-13983.

Dong, S., Wang, Y., Liu, Z., Zhang, W., Yi, K., Zhang, X., Zhang, X., Jiang, C., Yang, S., Wang, F., Xiao, X., 2020. Beehive-Inspired Macroporous SERS Probe for Cancer Detection through Capturing and Analyzing Exosomes in Plasma. ACS Appl Mater Interfaces 12(4), 5136-5146.

Dong, X., Chi, J., Zheng, L., Ma, B., Li, Z., Wang, S., Zhao, C., Liu, H., 2019b. Efficient isolation and sensitive quantification of extracellular vesicles based on an integrated ExoID-Chip using photonic crystals. Lab Chip 19(17), 2897-2904.

Doyle, L.M., Wang, M.Z., 2019. Overview of Extracellular Vesicles, Their Origin, Composition, Purpose, and Methods for Exosome Isolation and Analysis. Cells 8(7), 727.

Du, T., Yang, C.L., Ge, M.R., Liu, Y., Zhang, P., Li, H., Li, X.L., Li, T., Liu, Y.D., Dou, Y.C., Yang, B., Duan, R.S., 2020. M1 Macrophage Derived Exosomes Aggravate Experimental Autoimmune Neuritis via Modulating Th1 Response. Frontiers in Immunology 11, 1603.

Dudani, J.S., Gossett, D.R., Tse, H.T., Lamm, R.J., Kulkarni, R.P., Carlo, D.D., 2015. Rapid inertial solution exchange for enrichment and flow cytometric detection of microvesicles. Biomicrofluidics 9(1), 014112.

Everaert, C., Helsmoortel, H., Decock, A., Hulstaert, E., Van Paemel, R., Verniers, K., Nuytens, J., Anckaert, J., Nijs, N., Tulkens, J., Dhondt, B., Hendrix, A., Mestdagh, P., Vandesompele, J., 2019. Performance assessment of total RNA sequencing of human biofluids and extracellular vesicles. Sci Rep 9(1), 17574.

Fan, Y., Duan, X., Zhao, M., Wei, X., Wu, J., Chen, W., Liu, P., Cheng, W., Cheng, Q., Ding, S., 2020. High-sensitive and multiplex biosensing assay of NSCLC-derived exosomes via different recognition sites based on SPRi array. Biosens Bioelectron 154, 112066.

Fraire, J.C., Stremersch, S., Bouckaert, D., Monteyne, T., De Beer, T., Wuytens, P., De Rycke, R., Skirtach, A.G., Raemdonck, K., De Smedt, S., Braeckmans, K., 2019. Improved Label-Free Identification of Individual Exosome-like Vesicles with Au@Ag Nanoparticles as SERS Substrate. ACS Appl Mater Interfaces 11(43), 39424-39435.

Frankel, E.B., Audhya, A., 2018. ESCRT-dependent cargo sorting at multivesicular endosomes. Semin Cell Dev Biol 74, 4-10.

Giraldez, M.D., Spengler, R.M., Etheridge, A., Goicochea, A.J., Tuck, M., Choi, S.W., Galas, D.J., Tewari, M., 2019. Phospho-RNA-seq: a modified small RNA-seq method that reveals circulating mRNA and lncRNA fragments as potential biomarkers in human plasma. EMBO J 38(11), e101695.

Gori, A., Romanato, A., Greta, B., Strada, A., Gagni, P., Frigerio, R., Brambilla, D., Vago, R., Galbiati, S., Picciolini, S., Bedoni, M., Daaboul, G.G., Chiari, M., Cretich, M., 2020. Membrane-binding peptides for extracellular vesicles on-chip analysis. J Extracell Vesicles 9(1), 1751428.

Groen, K., Maltby, V.E., Scott, R.J., Tajouri, L., Lechner-Scott, J., 2020. Concentrations of plasma-borne extracellular particles differ between multiple sclerosis disease courses and compared to healthy controls. Mult Scler Relat Disord 45, 102446.

Gu, C., Bai, L., Pu, L., Gai, P., Li, F., 2021. Highly sensitive and stable self-powered biosensing for exosomes based on dual metal-organic frameworks nanocarriers. Biosens Bioelectron 176, 112907.

Guay, C., Jacovetti, C., Bayazit, M.B., Brozzi, F., Rodriguez-Trejo, A., Wu, K., Regazzi, R., 2020. Roles of noncoding RNAs in islet biology. Comprehensive Physiology 10(3), 893-932.

Guo, S., Xu, J., Estell, A.P., Ivory, C.F., Du, D., Lin, Y., Dong, W.J., 2020. Paper-based ITP technology: An application to specific cancer-derived exosome detection and analysis. Biosens Bioelectron 164, 112292.

Gurunathan, S., Kang, M.H., Jeyaraj, M., Qasim, M., Kim, J.H., 2019. Review of the Isolation, Characterization, Biological Function, and Multifarious Therapeutic Approaches of Exosomes. Cells 8(4), 307.

Guzman, N.A., Guzman, D.E., 2020. A Two-Dimensional Affinity Capture and Separation Mini-Platform for the Isolation, Enrichment, and Quantification of Biomarkers and Its Potential Use for Liquid Biopsy. Biomedicines 8(8), 255.

Hartjes, T.A., Mytnyk, S., Jenster, G.W., van Steijn, V., van Royen, M.E., 2019. Extracellular Vesicle Quantification and Characterization: Common Methods and Emerging Approaches. Bioengineering (Basel) 6(1), 7.

Hattori, Y., Shimada, T., Yasui, T., Kaji, N., Baba, Y., 2019. Micro- and Nanopillar Chips for Continuous Separation of Extracellular Vesicles. Anal Chem 91(10), 6514-6521.

He, F., Wang, J., Yin, B.C., Ye, B.C., 2018. Quantification of Exosome Based on a Copper-Mediated Signal Amplification Strategy. Anal Chem 90(13), 8072-8079.

He, M., Crow, J., Roth, M., Zeng, Y., Godwin, A.K., 2014. Integrated immunoisolation and protein analysis of circulating exosomes using microfluidic technology. Lab Chip 14(19), 3773-3780.

Hisey, C.L., Dorayappan, K.D.P., Cohn, D.E., Selvendiran, K., Hansford, D.J., 2018. Microfluidic affinity separation chip for selective capture and release of label-free ovarian cancer exosomes. Lab Chip 18(20), 3144-3153.

Horner, D.S., Pasini, M.E., Beltrame, M., Mastrodonato, V., Morelli, E., Vaccari, T., 2018. ESCRT genes and regulation of developmental signaling. Semin Cell Dev Biol 74, 29-39.

Hou, M., He, D., Bu, H., Wang, H., Huang, J., Gu, J., Wu, R., Li, H.W., He, X., Wang, K., 2020. A sandwich-type surface-enhanced Raman scattering sensor using dual aptamers and gold nanoparticles for the detection of tumor extracellular vesicles. Analyst 145(19), 6232-6236.

Hrdlickova, R., Toloue, M., Tian, B., 2017. RNA-Seq methods for transcriptome analysis. Wiley Interdiscip Rev RNA 8(1), e1364.

Huang, G., Lin, G., Zhu, Y., Duan, W., Jin, D., 2020a. Emerging technologies for profiling extracellular vesicle heterogeneity. Lab Chip 20(14), 2423-2437.

Huang, L., Wang, D.B., Singh, N., Yang, F., Gu, N., Zhang, X.E., 2018. A dual-signal amplification platform for sensitive fluorescence biosensing of leukemia-derived exosomes. Nanoscale 10(43), 20289-20295.

Huang, R., He, L., Li, S., Liu, H., Jin, L., Chen, Z., Zhao, Y., Li, Z., Deng, Y., He, N., 2020b. A simple fluorescence aptasensor for gastric cancer exosome detection based on branched rolling circle amplification. Nanoscale 12(4), 2445-2451.

Huang, R., He, L., Xia, Y., Xu, H., Liu, C., Xie, H., Wang, S., Peng, L., Liu, Y., Liu, Y., He, N., Li, Z., 2019. A Sensitive Aptasensor Based on a Hemin/G-Quadruplex-Assisted Signal Amplification Strategy for Electrochemical Detection of Gastric Cancer Exosomes. Small 15(19), e1900735.

Im, H., Shao, H., Park, Y.I., Peterson, V.M., Castro, C.M., Weissleder, R., Lee, H., 2014. Label-free detection and molecular profiling of exosomes with a nano-plasmonic sensor. Nat Biotechnol 32(5), 490-495.

Ishihara, R., Nakajima, T., Uchino, Y., Katagiri, A., Hosokawa, K., Maeda, M., Tomooka, Y., Kikuchi, A., 2017. Rapid and Easy Extracellular Vesicle Detection on a Surface-Functionalized Power-Free Microchip toward Point-of-Care Diagnostics. ACS Omega 2(10), 6703-6707.

Jalali, M., Isaac Hosseini, I., AbdelFatah, T., Montermini, L., Wachsmann Hogiu, S., Rak, J., Mahshid, S., 2021. Plasmonic nanobowtiefluidic device for sensitive detection of glioma extracellular vesicles by Raman spectrometry. Lab Chip 21(5), 855-866.

Jeong, S., Park, J., Pathania, D., Castro, C.M., Weissleder, R., Lee, H., 2016. Integrated Magneto-Electrochemical Sensor for Exosome Analysis. ACS Nano 10(2), 1802-1809.

Jiang, Y., Shi, M., Liu, Y., Wan, S., Cui, C., Zhang, L., Tan, W., 2017. Aptamer/AuNP Biosensor for Colorimetric Profiling of Exosomal Proteins. Angew Chem Int Ed Engl 56(39), 11916-11920.

Jin, D., Yang, F., Zhang, Y., Liu, L., Zhou, Y., Wang, F., Zhang, G.J., 2018. ExoAPP: Exosome-Oriented, Aptamer Nanoprobe-Enabled Surface Proteins Profiling and Detection. Anal Chem 90(24), 14402-14411.

Jorgensen, M., Baek, R., Pedersen, S., Sondergaard, E.K., Kristensen, S.R., Varming, K., 2013. Extracellular Vesicle (EV) Array: microarray capturing of exosomes and other extracellular vesicles for multiplexed phenotyping. J Extracell Vesicles 2.

Kabe, Y., Sakamoto, S., Hatakeyama, M., Yamaguchi, Y., Suematsu, M., Itonaga, M., Handa, H., 2019. Application of high-performance magnetic nanobeads to biological sensing devices. Anal Bioanal Chem 411(9), 1825-1837.

Kamyabi, N., Abbasgholizadeh, R., Maitra, A., Ardekani, A., Biswal, S.L., Grande-Allen, K.J., 2020. Isolation and mutational assessment of pancreatic cancer extracellular vesicles using a microfluidic platform. Biomed Microdevices 22(2), 23.

Kashefi-Kheyrabadi, L., Kim, J., Chakravarty, S., Park, S., Gwak, H., Kim, S.I., Mohammadniaei, M., Lee, M.H., Hyun, K.A., Jung, H.I., 2020. Detachable microfluidic device implemented with electrochemical aptasensor (DeMEA) for sequential analysis of cancerous exosomes. Biosens Bioelectron 169, 112622.

Kato, K., Kobayashi, M., Hanamura, N., Akagi, T., Kosaka, N., Ochiya, T., Ichiki, T., 2013. Electrokinetic Evaluation of Individual Exosomes by On-Chip Microcapillary Electrophoresis with Laser Dark-Field Microscopy. Japanese Journal of Applied Physics 52(6S), 06GK10.

Kawamura, A., Miyata, T., 2016. Biosensors, 157-176.

Kilic, T., Valinhas, A.T.S., Wall, I., Renaud, P., Carrara, S., 2018. Label-free detection of hypoxia-induced extracellular vesicle secretion from MCF-7 cells. Sci Rep 8(1), 9402.

Kulkarni, B., Kirave, P., Gondaliya, P., Jash, K., Jain, A., Tekade, R.K., Kalia, K., 2019. Exosomal miRNA in chemoresistance, immune evasion, metastasis and progression of cancer. Drug Discov Today 24(10), 2058-2067.

Kurian, T.K., Banik, S., Gopal, D., Chakrabarti, S., Mazumder, N., 2021. Elucidating Methods for Isolation and Quantification of Exosomes: A Review. Mol Biotechnol 63(4), 249-266.

Kwizera, E.A., O'Connor, R., Vinduska, V., Williams, M., Butch, E.R., Snyder, S.E., Chen, X., Huang, X., 2018. Molecular Detection and Analysis of Exosomes Using Surface-Enhanced Raman Scattering Gold Nanorods and a Miniaturized Device. Theranostics 8(10), 2722-2738.

Laki, A.J., Botzheim, L., Iván, K., Tamási, V., Civera, P., 2014. Separation of Microvesicles from Serological Samples Using Deterministic Lateral Displacement Effect. BioNanoScience 5(1), 48-54.

Lee, C., Carney, R., Lam, K., Chan, J.W., 2017. SERS analysis of selectively captured exosomes using an integrin-specific peptide ligand. J Raman Spectrosc 48(12), 1771-1776.

Lee, C., Carney, R.P., Hazari, S., Smith, Z.J., Knudson, A., Robertson, C.S., Lam, K.S., Wachsmann-Hogiu, S., 2015a. 3D plasmonic nanobowl platform for the study of exosomes in solution. Nanoscale 7(20), 9290-9297.

Lee, D., Wee, K.W., Kim, H., Han, S.I., Kwak, S., Yoon, D.S., Lee, J.H., 2020. Paper-Based Preconcentration and Isolation of Microvesicles and Exosomes. J Vis Exp(158).

Lee, K., Shao, H., Weissleder, R., Lee, H., 2015b. Acoustic purification of extracellular microvesicles. ACS Nano 9(3), 2321-2327.

Lennon, K.M., Wakefield, D.L., Maddox, A.L., Brehove, M.S., Willner, A.N., Garcia-Mansfield, K., Meechoovet, B., Reiman, R., Hutchins, E., Miller, M.M., Goel, A., Pirrotte, P., Van Keuren-Jensen, K., Jovanovic-Talisman, T., 2019. Single molecule characterization of individual extracellular vesicles from pancreatic cancer. J Extracell Vesicles 8(1), 1685634.

Li, B., Liu, C., Pan, W., Shen, J., Guo, J., Luo, T., Feng, J., Situ, B., An, T., Zhang, Y., Zheng, L., 2020. Facile fluorescent aptasensor using aggregation-induced emission luminogens for exosomal proteins profiling towards liquid biopsy. Biosens Bioelectron 168, 112520.

Li, Q., Tofaris, G.K., Davis, J.J., 2017. Concentration-Normalized Electroanalytical Assaying of Exosomal Markers. Anal Chem 89(5), 3184-3190.

Li, T.D., Zhang, R., Chen, H., Huang, Z.P., Ye, X., Wang, H., Deng, A.M., Kong, J.L., 2018. An ultrasensitive polydopamine bi-functionalized SERS immunoassay for exosome-based diagnosis and classification of pancreatic cancer. Chem Sci 9(24), 5372-5382.

Liao, G., Liu, X., Yang, X., Wang, Q., Geng, X., Zou, L., Liu, Y., Li, S., Zheng, Y., Wang, K., 2020. Surface plasmon resonance assay for exosomes based on aptamer recognition and polydopamine-functionalized gold nanoparticles for signal amplification. Microchim Acta 187(4), 251.

Liga, A., Vliegenthart, A.D., Oosthuyzen, W., Dear, J.W., Kersaudy-Kerhoas, M., 2015. Exosome isolation: a microfluidic road-map. Lab Chip 15(11), 2388-2394.

Lima Moura, S., Marti, M., Pividori, M.I., 2020. Matrix Effect in the Isolation of Breast Cancer-Derived Nanovesicles by Immunomagnetic Separation and Electrochemical Immunosensing-A Comparative Study. Sensors (Basel) 20(4), 965.

Linares, R., Tan, S., Gounou, C., Brisson, A.R., 2017. Imaging and Quantification of Extracellular Vesicles by Transmission Electron Microscopy. Methods Mol Biol 1545, 43-54.

Liu, C., Guo, J., Tian, F., Yang, N., Yan, F., Ding, Y., Wei, J., Hu, G., Nie, G., Sun, J., 2017. Field-Free Isolation of Exosomes from Extracellular Vesicles by Microfluidic Viscoelastic Flows. ACS Nano 11(7), 6968-6976.

Liu, C., Xu, X., Li, B., Situ, B., Pan, W., Hu, Y., An, T., Yao, S., Zheng, L., 2018a. Single-Exosome-Counting Immunoassays for Cancer Diagnostics. Nano Lett 18(7), 4226-4232.

Liu, C., Zhao, J., Tian, F., Chang, J., Zhang, W., Sun, J., 2019. lambda-DNA- and Aptamer-Mediated Sorting and Analysis of Extracellular Vesicles. J Am Chem Soc 141(9), 3817-3821.

Liu, W., Li, J., Wu, Y., Xing, S., Lai, Y., Zhang, G., 2018b. Target-induced proximity ligation triggers recombinase polymerase amplification and transcription-mediated amplification to detect tumor-derived exosomes in nasopharyngeal carcinoma with high sensitivity. Biosens Bioelectron 102, 204-210.

Lo, T.W., Zhu, Z., Purcell, E., Watza, D., Wang, J., Kang, Y.T., Jolly, S., Nagrath, D., Nagrath, S., 2020. Microfluidic device for high-throughput affinity-based isolation of extracellular vesicles. Lab Chip 20(10), 1762-1770.

Lotvall, J., Hill, A.F., Hochberg, F., Buzas, E.I., Di Vizio, D., Gardiner, C., Gho, Y.S., Kurochkin, I.V., Mathivanan, S., Quesenberry, P., Sahoo, S., Tahara, H., Wauben, M.H., Witwer, K.W., Thery, C., 2014. Minimal experimental requirements for definition of extracellular vesicles and their functions: a position statement from the International Society for Extracellular Vesicles. J Extracell Vesicles 3, 26913.

Maas, S.L., de Vrij, J., van der Vlist, E.J., Geragousian, B., van Bloois, L., Mastrobattista, E., Schiffelers, R.M., Wauben, M.H., Broekman, M.L., Nolte-'t Hoen, E.N., 2015. Possibilities and limitations of current technologies for quantification of biological extracellular vesicles and synthetic mimics. J Control Release 200, 87-96.

Maas, S.L.N., Breakefield, X.O., Weaver, A.M., 2017. Extracellular Vesicles: Unique Intercellular Delivery Vehicles. Trends Cell Biol 27(3), 172-188.

Maiolo, D., Paolini, L., Di Noto, G., Zendrini, A., Berti, D., Bergese, P., Ricotta, D., 2015. Colorimetric nanoplasmonic assay to determine purity and titrate extracellular vesicles. Anal Chem 87(8), 4168-4176.

Mathew, D.G., Beekman, P., Lemay, S.G., Zuilhof, H., Le Gac, S., van der Wiel, W.G., 2020. Electrochemical Detection of Tumor-Derived Extracellular Vesicles on Nanointerdigitated Electrodes. Nano Lett 20(2), 820-828.

Mathieu, M., Martin-Jaular, L., Lavieu, G., Thery, C., 2019. Specificities of secretion and uptake of exosomes and other extracellular vesicles for cell-to-cell communication. Nat Cell Biol 21(1), 9-17.

Melo, S.A., Sugimoto, H., O'Connell, J.T., Kato, N., Villanueva, A., Vidal, A., Qiu, L., Vitkin, E., Perelman, L.T., Melo, C.A., Lucci, A., Ivan, C., Calin, G.A., Kalluri, R., 2014. Cancer exosomes perform cell-independent microRNA biogenesis and promote tumorigenesis. Cancer Cell 26(5), 707-721.

Merdalimova, A., Chernyshev, V., Nozdriukhin, D., Rudakovskaya, P., Gorin, D., Yashchenok, A., 2019. Identification and Analysis of Exosomes by Surface-Enhanced Raman Spectroscopy. Applied Sciences 9(6), 1135.

Min, J., Son, T., Hong, J.S., Cheah, P.S., Wegemann, A., Murlidharan, K., Weissleder, R., Lee, H., Im, H., 2020. Plasmon-Enhanced Biosensing for Multiplexed Profiling of Extracellular Vesicles. Adv Biosyst 4, 2000003.

Minciacchi, V.R., Freeman, M.R., Di Vizio, D., 2015. Extracellular vesicles in cancer: exosomes, microvesicles and the emerging role of large oncosomes. Semin Cell Dev Biol 40, 41-51.

Mirtaheri, E., Dolatmoradi, A., El-Zahab, B., 2019. Thermally Assisted Acoustofluidic Separation Based on Membrane Protein Content. Anal Chem 91(21), 13953-13961.

Momen-Heravi, F., Getting, S.J., Moschos, S.A., 2018. Extracellular vesicles and their nucleic acids for biomarker discovery. Pharmacol Ther 192, 170-187.

Monošík, R., Streďanský, M., Šturdík, E., 2012. Biosensors - classification, characterization and new trends. Acta Chimica Slovaca 5(1), 109-120.

Morani, M., Mai, T.D., Krupova, Z., Defrenaix, P., Multia, E., Riekkola, M.L., Taverna, M., 2020. Electrokinetic characterization of extracellular vesicles with capillary electrophoresis: A new tool for their identification and quantification. Anal Chim Acta 1128, 42-51.

Mori, K., Hirase, M., Morishige, T., Takano, E., Sunayama, H., Kitayama, Y., Inubushi, S., Sasaki, R., Yashiro, M., Takeuchi, T., 2019. A Pretreatment-Free, Polymer-Based Platform Prepared by Molecular Imprinting and Post-Imprinting Modifications for Sensing Intact Exosomes. Angew Chem Int Ed Engl 58(6), 1612-1615.

Moyano, A., Serrano-Pertierra, E., Salvador, M., Martinez-Garcia, J.C., Pineiro, Y., Yanez-Vilar, S., Gonzalez-Gomez, M., Rivas, J., Rivas, M., Blanco-Lopez, M.C., 2020. Carbon-Coated Superparamagnetic Nanoflowers for Biosensors Based on Lateral Flow Immunoassays. Biosensors (Basel) 10(8), 80.

Nakamura, K., Kusama, K., Suda, Y., Fujiwara, H., Hori, M., Imakawa, K., 2020. Emerging role of extracellular vesicles in embryo–maternal communication throughout implantation processes. International Journal of Molecular Sciences 21(15), 1-15.

Ning, C.F., Wang, L., Tian, Y.F., Yin, B.C., Ye, B.C., 2020. Multiple and sensitive SERS detection of cancer-related exosomes based on gold-silver bimetallic nanotrepangs. Analyst 145(7), 2795-2804.

Oliveira-Rodriguez, M., Lopez-Cobo, S., Reyburn, H.T., Costa-Garcia, A., Lopez-Martin, S., Yanez-Mo, M., Cernuda-Morollon, E., Paschen, A., Vales-Gomez, M., Blanco-Lopez, M.C., 2016. Development of a rapid lateral flow immunoassay test for detection of exosomes previously enriched from cell culture medium and body fluids. J Extracell Vesicles 5, 31803.

Ouahabi, O.E., Salim, H., Pero-Gascon, R., Benavente, F., 2021. A simple method for the analysis of extracellular vesicles enriched for exosomes from human serum by capillary electrophoresis with ultraviolet diode array detection. J Chromatogr A 1635, 461752.

Park, J., Lin, H.Y., Assaker, J.P., Jeong, S., Huang, C.H., Kurdi, T., Lee, K., Fraser, K., Min, C., Eskandari, S., Routray, S., Tannous, B., Abdi, R., Riella, L., Chandraker, A., Castro, C.M., Weissleder, R., Lee, H., Azzi, J.R., 2017. Integrated Kidney Exosome Analysis for the Detection of Kidney Transplant Rejection. ACS Nano 11(11), 11041-11046.

Picciolini, S., Gualerzi, A., Vanna, R., Sguassero, A., Gramatica, F., Bedoni, M., Masserini, M., Morasso, C., 2018. Detection and Characterization of Different Brain-Derived Subpopulations of Plasma Exosomes by Surface Plasmon Resonance Imaging. Anal Chem 90(15), 8873-8880.

Pirzada, M., Altintas, Z., 2019. Nanomaterials for Healthcare Biosensing Applications. Sensors (Basel) 19(23), 5311.

Qiu, G., Thakur, A., Xu, C., Ng, S.-P., Lee, Y., Wu, C.-M.L., 2019. Detection of Glioma-Derived Exosomes with the Biotinylated Antibody-Functionalized Titanium Nitride Plasmonic Biosensor. Advanced Functional Materials 29(9), 1806761.

Reategui, E., van der Vos, K.E., Lai, C.P., Zeinali, M., Atai, N.A., Aldikacti, B., Floyd, F.P., Jr., A, H.K., Thapar, V., Hochberg, F.H., Sequist, L.V., Nahed, B.V., B, S.C., Toner, M., Balaj, L., D, T.T., Breakefield, X.O., Stott, S.L., 2018. Engineered nanointerfaces for microfluidic isolation and molecular profiling of tumor-specific extracellular vesicles. Nat Commun 9(1), 175.

Reiner, A.T., Ferrer, N.G., Venugopalan, P., Lai, R.C., Lim, S.K., Dostalek, J., 2017a. Magnetic nanoparticle-enhanced surface plasmon resonance biosensor for extracellular vesicle analysis. Analyst 142(20), 3913-3921.

Reiner, A.T., Tan, S., Agreiter, C., Auer, K., Bachmayr-Heyda, A., Aust, S., Pecha, N., Mandorfer, M., Pils, D., Brisson, A.R., Zeillinger, R., Lim, S.K., 2017b. EV-Associated MMP9 in High-Grade Serous Ovarian Cancer Is Preferentially Localized to Annexin V-Binding EVs. Dis Markers 2017, 9653194.

Rojalin, T., Koster, H.J., Liu, J., Mizenko, R.R., Tran, D., Wachsmann-Hogiu, S., Carney, R.P., 2020. Hybrid Nanoplasmonic Porous Biomaterial Scaffold for Liquid Biopsy Diagnostics Using Extracellular Vesicles. ACS Sens 5(9), 2820-2833.

Rojas, C., Campos-Mora, M., Cárcamo, I., Villalón, N., Elhusseiny, A., Contreras-Kallens, P., Refisch, A., Gálvez-Jirón, F., Emparán, I., Montoya-Riveros, A., Vernal, R., Pino-Lagos, K., 2020. T regulatory cells-derived extracellular vesicles and their contribution to the generation of immune tolerance. Journal of Leukocyte Biology 108(3), 813-824.

Romanszki, L., Varga, Z., Mihaly, J., Keresztes, Z., Thompson, M., 2020. Electromagnetic Piezoelectric Acoustic Sensor Detection of Extracellular Vesicles through Interaction with Detached Vesicle Proteins. Biosensors (Basel) 10(11).

Rupert, D.L.M., Claudio, V., Lasser, C., Bally, M., 2017. Methods for the physical characterization and quantification of extracellular vesicles in biological samples. Biochim Biophys Acta Gen Subj 1861(1 Pt A), 3164-3179.

Rupert, D.L.M., Shelke, G.V., Emilsson, G., Claudio, V., Block, S., Lasser, C., Dahlin, A., Lotvall, J.O., Bally, M., Zhdanov, V.P., Hook, F., 2016. Dual-Wavelength Surface Plasmon Resonance for Determining the Size and Concentration of Sub-Populations of Extracellular Vesicles. Anal Chem 88(20), 9980-9988.

Salafi, T., Zhang, Y., Zhang, Y., 2019. A Review on Deterministic Lateral Displacement for Particle Separation and Detection. Nano-Micro Letters 11(1).

Santana, S.M., Antonyak, M.A., Cerione, R.A., Kirby, B.J., 2014. Microfluidic isolation of cancer-cell-derived microvesicles from hetergeneous extracellular shed vesicle populations. Biomed Microdevices 16(6), 869-877.

Shao, H., Chung, J., Balaj, L., Charest, A., Bigner, D.D., Carter, B.S., Hochberg, F.H., Breakefield, X.O., Weissleder, R., Lee, H., 2012. Protein typing of circulating microvesicles allows real-time monitoring of glioblastoma therapy. Nat Med 18(12), 1835-1840.

Shao, H., Im, H., Castro, C.M., Breakefield, X., Weissleder, R., Lee, H., 2018. New Technologies for Analysis of Extracellular Vesicles. Chem Rev 118(4), 1917-1950.

Shi, L., Kuhnell, D., Borra, V.J., Langevin, S.M., Nakamura, T., Esfandiari, L., 2019. Rapid and label-free isolation of small extracellular vesicles from biofluids utilizing a novel insulator based dielectrophoretic device. Lab Chip 19(21), 3726-3734.

Sina, A.A., Vaidyanathan, R., Dey, S., Carrascosa, L.G., Shiddiky, M.J., Trau, M., 2016. Real time and label free profiling of clinically relevant exosomes. Sci Rep 6, 30460.

Sivashanmugan, K., Huang, W.-L., Lin, C.-H., Liao, J.-D., Lin, C.-C., Su, W.-C., Wen, T.-C., 2017. Bimetallic nanoplasmonic gap-mode SERS substrate for lung normal and cancer-derived exosomes detection. Journal of the Taiwan Institute of Chemical Engineers 80, 149-155.

Smith, J.T., Wunsch, B.H., Dogra, N., Ahsen, M.E., Lee, K., Yadav, K.K., Weil, R., Pereira, M.A., Patel, J.V., Duch, E.A., Papalia, J.M., Lofaro, M.F., Gupta, M., Tewari, A.K., Cordon-Cardo, C., Stolovitzky, G., Gifford, S.M., 2018. Integrated nanoscale deterministic lateral displacement arrays for separation of extracellular vesicles from clinically-relevant volumes of biological samples. Lab Chip 18(24), 3913-3925.

Soung, Y.H., Nguyen, T., Cao, H., Lee, J., Chung, J., 2016. Emerging roles of exosomes in cancer invasion and metastasis. BMB Rep 49(1), 18-25.

Stahl, P.D., Raposo, G., 2018. Exosomes and extracellular vesicles: the path forward. Essays Biochem 62(2), 119-124.

Stam, J., Bartel, S., Bischoff, R., Wolters, J.C., 2021. Isolation of extracellular vesicles with combined enrichment methods. J Chromatogr B Analyt Technol Biomed Life Sci 1169, 122604.

Stremersch, S., Marro, M., Pinchasik, B.E., Baatsen, P., Hendrix, A., De Smedt, S.C., Loza-Alvarez, P., Skirtach, A.G., Raemdonck, K., Braeckmans, K., 2016. Identification of Individual Exosome-Like Vesicles by Surface Enhanced Raman Spectroscopy. Small 12(24), 3292-3301.

Sun, N., Lee, Y.T., Zhang, R.Y., Kao, R., Teng, P.C., Yang, Y., Yang, P., Wang, J.J., Smalley, M., Chen, P.J., Kim, M., Chou, S.J., Bao, L., Wang, J., Zhang, X., Qi, D., Palomique, J., Nissen, N., Han, S.B., Sadeghi, S., Finn, R.S., Saab, S., Busuttil, R.W., Markovic, D., Elashoff, D., Yu, H.H., Li, H., Heaney, A.P., Posadas, E., You, S., Yang, J.D., Pei, R., Agopian, V.G., Tseng, H.R., Zhu, Y., 2020. Purification of HCC-specific extracellular vesicles on nanosubstrates for early HCC detection by digital scoring. Nat Commun 11(1), 4489.

Sung, B.H., Weaver, A.M., 2017. Exosome secretion promotes chemotaxis of cancer cells. Cell Adh Migr 11(2), 187-195.

Sunkara, V., Woo, H.K., Cho, Y.K., 2016. Emerging techniques in the isolation and characterization of extracellular vesicles and their roles in cancer diagnostics and prognostics. Analyst 141(2), 371-381.

Suthar, J., Parsons, E.S., Hoogenboom, B.W., Williams, G.R., Guldin, S., 2020. Acoustic Immunosensing of Exosomes Using a Quartz Crystal Microbalance with Dissipation Monitoring. Anal Chem 92(5), 4082-4093.

Suwatthanarak, T., Thiodorus, I.A., Tanaka, M., Shimada, T., Takeshita, D., Yasui, T., Baba, Y., Okochi, M., 2021. Microfluidic-based capture and release of cancer-derived exosomes via peptide-nanowire hybrid interface. Lab Chip 21(3), 597-607.

Takeuchi, T., Mori, K., Sunayama, H., Takano, E., Kitayama, Y., Shimizu, T., Hirose, Y., Inubushi, S., Sasaki, R., Tanino, H., 2020. Antibody-Conjugated Signaling Nanocavities Fabricated by Dynamic Molding for Detecting Cancers Using Small Extracellular Vesicle Markers from Tears. J Am Chem Soc 142(14), 6617-6624.

Tayebi, M., Tavakkoli Yaraki, M., Yang, H.Y., Ai, Y., 2019. A MoS2–MWCNT based fluorometric nanosensor for exosome detection and quantification. Nanoscale Advances 1(8), 2866-2872.

Tayebi, M., Zhou, Y., Tripathi, P., Chandramohanadas, R., Ai, Y., 2020. Exosome Purification and Analysis Using a Facile Microfluidic Hydrodynamic Trapping Device. Anal Chem 92(15), 10733-10742.

Thakur, A., Qiu, G., Ng, S.P., Guan, J., Yue, J., Lee, Y., Wu, C.L., 2017. Direct detection of two different tumor-derived extracellular vesicles by SAM-AuNIs LSPR biosensor. Biosens Bioelectron 94, 400-407.

Thery, C., Witwer, K.W., Aikawa, E., Alcaraz, M.J., Anderson, J.D., Andriantsitohaina, R., Antoniou, A., Arab, T., Archer, F., Atkin-Smith, G.K., Ayre, D.C., Bach, J.M., Bachurski, D., Baharvand, H., Balaj, L., Baldacchino, S., Bauer, N.N., Baxter, A.A., Bebawy, M., Beckham, C., Bedina Zavec, A., Benmoussa, A., Berardi, A.C., Bergese, P., Bielska, E., Blenkiron, C., Bobis-Wozowicz, S., Boilard, E., Boireau, W., Bongiovanni, A., Borras, F.E., Bosch, S., Boulanger, C.M., Breakefield, X., Breglio, A.M., Brennan, M.A., Brigstock, D.R., Brisson, A., Broekman, M.L., Bromberg, J.F., Bryl-Gorecka, P., Buch, S., Buck, A.H., Burger, D., Busatto, S., Buschmann, D., Bussolati, B., Buzas, E.I., Byrd, J.B., Camussi, G., Carter, D.R., Caruso, S., Chamley, L.W., Chang, Y.T., Chen, C., Chen, S., Cheng, L., Chin, A.R., Clayton, A., Clerici, S.P., Cocks, A., Cocucci, E., Coffey, R.J., Cordeiro-da-Silva, A., Couch, Y., Coumans, F.A., Coyle, B., Crescitelli, R., Criado, M.F., D'Souza-Schorey, C., Das, S., Datta Chaudhuri, A., de Candia, P., De Santana, E.F., De Wever, O., Del Portillo, H.A., Demaret, T., Deville, S., Devitt, A., Dhondt, B., Di Vizio, D., Dieterich, L.C., Dolo, V., Dominguez Rubio, A.P., Dominici, M., Dourado, M.R., Driedonks, T.A., Duarte, F.V., Duncan, H.M., Eichenberger, R.M., Ekstrom, K., El Andaloussi, S., Elie-Caille, C., Erdbrugger, U., Falcon-Perez, J.M., Fatima, F., Fish, J.E., Flores-Bellver, M., Forsonits, A., Frelet-Barrand, A., Fricke, F., Fuhrmann, G., Gabrielsson, S., Gamez-Valero, A., Gardiner, C., Gartner, K., Gaudin, R., Gho, Y.S., Giebel, B., Gilbert, C., Gimona, M., Giusti, I., Goberdhan, D.C., Gorgens, A., Gorski, S.M., Greening, D.W., Gross, J.C., Gualerzi, A., Gupta, G.N., Gustafson, D., Handberg, A., Haraszti, R.A., Harrison, P., Hegyesi, H., Hendrix, A., Hill, A.F., Hochberg, F.H., Hoffmann, K.F., Holder, B., Holthofer, H., Hosseinkhani, B., Hu, G., Huang, Y., Huber, V., Hunt, S., Ibrahim, A.G., Ikezu, T., Inal, J.M., Isin, M., Ivanova, A., Jackson, H.K., Jacobsen, S., Jay, S.M., Jayachandran, M., Jenster, G., Jiang, L., Johnson, S.M., Jones, J.C., Jong, A., Jovanovic-Talisman, T., Jung, S., Kalluri, R., Kano, S.I., Kaur, S., Kawamura, Y., Keller, E.T., Khamari, D., Khomyakova, E., Khvorova, A., Kierulf, P., Kim, K.P., Kislinger, T., Klingeborn, M., Klinke, D.J., 2nd, Kornek, M., Kosanovic, M.M., Kovacs, A.F., Kramer-Albers, E.M., Krasemann, S., Krause, M., Kurochkin, I.V., Kusuma, G.D., Kuypers, S., Laitinen, S., Langevin, S.M., Languino, L.R., Lannigan, J., Lasser, C., Laurent, L.C., Lavieu, G., Lazaro-Ibanez, E., Le Lay, S., Lee, M.S., Lee, Y.X.F., Lemos, D.S., Lenassi, M., Leszczynska, A., Li, I.T., Liao, K., Libregts, S.F., Ligeti, E., Lim, R., Lim, S.K., Line, A., Linnemannstons, K., Llorente, A., Lombard, C.A., Lorenowicz, M.J., Lorincz, A.M., Lotvall, J., Lovett, J., Lowry, M.C., Loyer, X., Lu, Q., Lukomska, B., Lunavat, T.R., Maas, S.L., Malhi, H., Marcilla, A., Mariani, J., Mariscal, J., Martens-Uzunova, E.S., Martin-Jaular, L., Martinez, M.C., Martins, V.R., Mathieu, M., Mathivanan, S., Maugeri, M., McGinnis, L.K., McVey, M.J., Meckes, D.G., Jr., Meehan, K.L., Mertens, I., Minciacchi, V.R., Moller, A., Moller Jorgensen, M., Morales-Kastresana, A., Morhayim, J., Mullier, F., Muraca, M., Musante, L., Mussack, V., Muth, D.C., Myburgh, K.H., Najrana, T., Nawaz, M., Nazarenko, I., Nejsum, P., Neri, C., Neri, T., Nieuwland, R., Nimrichter, L., Nolan, J.P., Nolte-'t Hoen, E.N., Noren Hooten, N., O'Driscoll, L., O'Grady, T., O'Loghlen, A., Ochiya, T., Olivier, M., Ortiz, A., Ortiz, L.A., Osteikoetxea, X., Ostergaard, O., Ostrowski, M., Park, J., Pegtel, D.M., Peinado, H., Perut, F., Pfaffl, M.W., Phinney, D.G., Pieters, B.C., Pink, R.C., Pisetsky, D.S., Pogge von Strandmann, E., Polakovicova, I., Poon, I.K., Powell, B.H., Prada, I., Pulliam, L., Quesenberry, P., Radeghieri, A., Raffai, R.L., Raimondo, S., Rak, J., Ramirez, M.I., Raposo, G., Rayyan, M.S., Regev-Rudzki, N., Ricklefs, F.L., Robbins, P.D., Roberts, D.D., Rodrigues, S.C., Rohde, E., Rome, S., Rouschop, K.M., Rughetti, A., Russell, A.E., Saa, P., Sahoo, S., Salas-Huenuleo, E., Sanchez, C., Saugstad, J.A., Saul, M.J., Schiffelers, R.M., Schneider, R., Schoyen,

T.H., Scott, A., Shahaj, E., Sharma, S., Shatnyeva, O., Shekari, F., Shelke, G.V., Shetty, A.K., Shiba, K., Siljander, P.R., Silva, A.M., Skowronek, A., Snyder, O.L., 2nd, Soares, R.P., Sodar, B.W., Soekmadji, C., Sotillo, J., Stahl, P.D., Stoorvogel, W., Stott, S.L., Strasser, E.F., Swift, S., Tahara, H., Tewari, M., Timms, K., Tiwari, S., Tixeira, R., Tkach, M., Toh, W.S., Tomasini, R., Torrecilhas, A.C., Tosar, J.P., Toxavidis, V., Urbanelli, L., Vader, P., van Balkom, B.W., van der Grein, S.G., Van Deun, J., van Herwijnen, M.J., Van Keuren-Jensen, K., van Niel, G., van Royen, M.E., van Wijnen, A.J., Vasconcelos, M.H., Vechetti, I.J., Jr., Veit, T.D., Vella, L.J., Velot, E., Verweij, F.J., Vestad, B., Vinas, J.L., Visnovitz, T., Vukman, K.V., Wahlgren, J., Watson, D.C., Wauben, M.H., Weaver, A., Webber, J.P., Weber, V., Wehman, A.M., Weiss, D.J., Welsh, J.A., Wendt, S., Wheelock, A.M., Wiener, Z., Witte, L., Wolfram, J., Xagorari, A., Xander, P., Xu, J., Yan, X., Yanez-Mo, M., Yin, H., Yuana, Y., Zappulli, V., Zarubova, J., Zekas, V., Zhang, J.Y., Zhao, Z., Zheng, L., Zheutlin, A.R., Zickler, A.M., Zimmermann, P., Zivkovic, A.M., Zocco, D., Zuba-Surma, E.K., 2018. Minimal information for studies of extracellular vesicles 2018 (MISEV2018): a position statement of the International Society for Extracellular Vesicles and update of the MISEV2014 guidelines. J Extracell Vesicles 7(1), 1535750.

Tian, Y.F., Ning, C.F., He, F., Yin, B.C., Ye, B.C., 2018. Highly sensitive detection of exosomes by SERS using gold nanostar@Raman reporter@nanoshell structures modified with a bivalent cholesterol-labeled DNA anchor. Analyst 143(20), 4915-4922.

Tirinato, L., Gentile, F., Di Mascolo, D., Coluccio, M.L., Das, G., Liberale, C., Pullano, S.A., Perozziello, G., Francardi, M., Accardo, A., De Angelis, F., Candeloro, P., Di Fabrizio, E., 2012. SERS analysis on exosomes using super-hydrophobic surfaces. Microelectronic Engineering 97, 337-340.

Trivedi, M.S., Abreu, M., 2018. Nucleic Acid Profiling in Tumor Exosomes, Elsevier Academic Press, 93-117.

van der Pol, E., Boing, A.N., Gool, E.L., Nieuwland, R., 2016. Recent developments in the nomenclature, presence, isolation, detection and clinical impact of extracellular vesicles. J Thromb Haemost 14(1), 48-56.

van der Pol, E., Coumans, F.A., Grootemaat, A.E., Gardiner, C., Sargent, I.L., Harrison, P., Sturk, A., van Leeuwen, T.G., Nieuwland, R., 2014. Particle size distribution of exosomes and microvesicles determined by transmission electron microscopy, flow cytometry, nanoparticle tracking analysis, and resistive pulse sensing. J Thromb Haemost 12(7), 1182-1192.

van Niel, G., D'Angelo, G., Raposo, G., 2018. Shedding light on the cell biology of extracellular vesicles. Nat Rev Mol Cell Biol 19(4), 213-228.

Wang, C., Wang, C., Jin, D., Yu, Y., Yang, F., Zhang, Y., Yao, Q., Zhang, G.J., 2020a. AuNP-Amplified Surface Acoustic Wave Sensor for the Quantification of Exosomes. ACS Sens 5(2), 362-369.

Wang, H., Wan, K., Zhou, Y., He, X., He, D., Cheng, H., Huang, J., Jia, R., Wang, K., 2020b. A three-dimensional multipedal DNA walker for the ultrasensitive detection of tumor exosomes. Chem Commun (Camb) 56(85), 12949-12952.

Wang, J., Wuethrich, A., Sina, A.A., Lane, R.E., Lin, L.L., Wang, Y., Cebon, J., Behren, A., Trau, M., 2020c. Tracking extracellular vesicle phenotypic changes enables treatment monitoring in melanoma. Sci Adv 6(9), eaax3223.

Wang, L., Zeng, L., Wang, Y., Chen, T., Chen, W., Chen, G., Li, C., Chen, J., 2021a. Electrochemical aptasensor based on multidirectional hybridization chain reaction for detection of tumorous exosomes. Sens Actuators B Chem 332, 129471.

Wang, M., Pan, Y., Wu, S., Sun, Z., Wang, L., Yang, J., Yin, Y., Li, G., 2020d. Detection of colorectal cancer-derived exosomes based on covalent organic frameworks. Biosens Bioelectron 169, 112638.

Wang, S., Zhang, L., Wan, S., Cansiz, S., Cui, C., Liu, Y., Cai, R., Hong, C., Teng, I.T., Shi, M., Wu, Y., Dong, Y., Tan, W., 2017a. Aptasensor with Expanded Nucleotide Using DNA Nanotetrahedra for Electrochemical Detection of Cancerous Exosomes. ACS Nano 11(4), 3943-3949.

Wang, X., Yuan, X., Fu, K., Liu, C., Bai, L., Wang, X., Tan, X., Zhang, Y., 2021b. Colorimetric analysis of extracellular vesicle surface proteins based on controlled growth of Au aptasensors. Analyst 146(6), 2019-2028.

Wang, Y., Li, Q., Shi, H., Tang, K., Qiao, L., Yu, G., Ding, C., Yu, S., 2020e. Microfluidic Raman biochip detection of exosomes: a promising tool for prostate cancer diagnosis. Lab Chip 20(24), 4632-4637.

Wang, Y., Yuan, W., Kimber, M., Lu, M., Dong, L., 2018a. Rapid Differentiation of Host and Parasitic Exosome Vesicles Using Microfluidic Photonic Crystal Biosensor. ACS Sens 3(9), 1616-1621.

Wang, Y., Zhang, Q., Yuan, W., Wang, Y., Loghry, H.J., Zhao, Z., Kimber, M.J., Dong, L., Lu, M., 2021c. Hyperspectral imaging-based exosome microarray for rapid molecular profiling of extracellular vesicles. Lab Chip 21(1), 196-204.

Wang, Y.M., Liu, J.W., Adkins, G.B., Shen, W., Trinh, M.P., Duan, L.Y., Jiang, J.H., Zhong, W., 2017b. Enhancement of the Intrinsic Peroxidase-Like Activity of Graphitic Carbon Nitride Nanosheets by ssDNAs and Its Application for Detection of Exosomes. Anal Chem 89(22), 12327-12333.

Wang, Z., Li, F., Rufo, J., Chen, C., Yang, S., Li, L., Zhang, J., Cheng, J., Kim, Y., Wu, M., Abemayor, E., Tu, M., Chia, D., Spruce, R., Batis, N., Mehanna, H., Wong, D.T.W., Huang, T.J., 2020f. Acoustofluidic Salivary Exosome Isolation: A Liquid Biopsy Compatible Approach for Human Papillomavirus-Associated Oropharyngeal Cancer Detection. J Mol Diagn 22(1), 50-59.

Wang, Z., Sun, X., Natalia, A., Tang, C.S.L., Ang, C.B.T., Ong, C.-A.J., Teo, M.C.C., So, J.B.Y., Shao, H., 2020g. Dual-Selective Magnetic Analysis of Extracellular Vesicle Glycans. Matter 2(1), 150-166.

Wang, Z., Wu, H.J., Fine, D., Schmulen, J., Hu, Y., Godin, B., Zhang, J.X., Liu, X., 2013. Ciliated micropillars for the microfluidic-based isolation of nanoscale lipid vesicles. Lab Chip 13(15), 2879-2882.

Wang, Z., Zong, S., Wang, Y., Li, N., Li, L., Lu, J., Wang, Z., Chen, B., Cui, Y., 2018b. Screening and multiple detection of cancer exosomes using an SERS-based method. Nanoscale 10(19), 9053-9062.

Wu, M., Chen, C., Wang, Z., Bachman, H., Ouyang, Y., Huang, P.H., Sadovsky, Y., Huang, T.J., 2019. Separating extracellular vesicles and lipoproteins via acoustofluidics. Lab Chip 19(7), 1174-1182.

Wu, M., Chen, Z., Xie, Q., Xiao, B., Zhou, G., Chen, G., Bian, Z., 2021. One-step quantification of salivary exosomes based on combined aptamer recognition and quantum dot signal amplification. Biosens Bioelectron 171, 112733.

Wu, M., Ouyang, Y., Wang, Z., Zhang, R., Huang, P.H., Chen, C., Li, H., Li, P., Quinn, D., Dao, M., Suresh, S., Sadovsky, Y., Huang, T.J., 2017. Isolation of exosomes from whole blood by integrating acoustics and microfluidics. Proc Natl Acad Sci U S A 114(40), 10584-10589.

Wunsch, B.H., Smith, J.T., Gifford, S.M., Wang, C., Brink, M., Bruce, R.L., Austin, R.H., Stolovitzky, G., Astier, Y., 2016. Nanoscale lateral displacement arrays for the separation of exosomes and colloids down to 20 nm. Nat Nanotechnol 11(11), 936-940.

Xia, Y., Chen, T., Chen, G., Weng, Y., Zeng, L., Liao, Y., Chen, W., Lan, J., Zhang, J., Chen, J., 2020. A nature-inspired colorimetric and fluorescent dual-modal biosensor for exosomes detection. Talanta 214, 120851.

Xia, Y., Liu, M., Wang, L., Yan, A., He, W., Chen, M., Lan, J., Xu, J., Guan, L., Chen, J., 2017. A visible and colorimetric aptasensor based on DNA-capped single-walled carbon nanotubes for detection of exosomes. Biosens Bioelectron 92, 8-15.

Xu, H., Liao, C., Zuo, P., Liu, Z., Ye, B.C., 2018. Magnetic-Based Microfluidic Device for On-Chip Isolation and Detection of Tumor-Derived Exosomes. Anal Chem 90(22), 13451-13458.

Xu, H., Yao, J., Wu, D.C., Lambowitz, A.M., 2019. Improved TGIRT-seq methods for comprehensive transcriptome profiling with decreased adapter dimer formation and bias correction. Sci Rep 9(1), 7953.

Xu, L., Chopdat, R., Li, D., Al-Jamal, K.T., 2020. Development of a simple, sensitive and selective colorimetric aptasensor for the detection of cancer-derived exosomes. Biosens Bioelectron 169, 112576.

Yadav, S., Boriachek, K., Islam, M.N., Lobb, R., Möller, A., Hill, M.M., Hossain, M.S.A., Nguyen, N.-T., Shiddiky, M.J.A., 2017. An Electrochemical Method for the Detection of Disease-Specific Exosomes. ChemElectroChem 4(4), 967-971.

Yan, Z., Dutta, S., Liu, Z., Yu, X., Mesgarzadeh, N., Ji, F., Bitan, G., Xie, Y.H., 2019. A Label-Free Platform for Identification of Exosomes from Different Sources. ACS Sens 4(2), 488-497.

Yanez-Mo, M., Siljander, P.R., Andreu, Z., Zavec, A.B., Borras, F.E., Buzas, E.I., Buzas, K., Casal, E., Cappello, F., Carvalho, J., Colas, E., Cordeiro-da Silva, A., Fais, S., Falcon-Perez, J.M., Ghobrial, I.M., Giebel, B., Gimona, M., Graner, M., Gursel, I., Gursel, M., Heegaard, N.H., Hendrix, A., Kierulf, P., Kokubun, K., Kosanovic, M., Kralj-Iglic, V., Kramer-Albers, E.M., Laitinen, S., Lasser, C., Lener, T., Ligeti, E., Line, A., Lipps, G., Llorente, A., Lotvall, J., Mancek-Keber, M., Marcilla, A., Mittelbrunn, M., Nazarenko, I., Nolte-'t Hoen, E.N., Nyman, T.A., O'Driscoll, L., Olivan, M., Oliveira, C., Pallinger, E., Del Portillo, H.A., Reventos, J., Rigau, M., Rohde, E., Sammar, M., Sanchez-Madrid, F., Santarem, N., Schallmoser, K., Ostenfeld, M.S., Stoorvogel, W., Stukelj, R., Van der Grein, S.G., Vasconcelos, M.H., Wauben, M.H., De Wever, O., 2015. Biological properties of extracellular vesicles and their physiological functions. J Extracell Vesicles 4, 27066.

Yang, Y., Li, C., Shi, H., Chen, T., Wang, Z., Li, G., 2019. A pH-responsive bioassay for paper-based diagnosis of exosomes via mussel-inspired surface chemistry. Talanta 192, 325-330.

Yang, Y., Ye, Y., Su, X., He, J., Bai, W., He, X., 2017. MSCs-Derived Exosomes and Neuroinflammation, Neurogenesis and Therapy of Traumatic Brain Injury. Front Cell Neurosci 11, 55.

Yang, Y., Zhai, C., Zeng, Q., Khan, A.L., Yu, H., 2020. Multifunctional Detection of Extracellular Vesicles with Surface Plasmon Resonance Microscopy. Anal Chem 92(7), 4884-4890.

Yasui, T., Yanagida, T., Ito, S., Konakade, Y., Takeshita, D., Naganawa, T., Nagashima, K., Shimada, T., Kaji, N., Nakamura, Y., Thiodorus, I.A., He, Y., Rahong, S., Kanai, M., Yukawa, H., Ochiya, T., Kawai, T., Baba, Y., 2017. Unveiling massive numbers of cancer-related urinary-microRNA candidates via nanowires. Sci Adv 3(12), e1701133.

Yildizhan, Y., Vajrala, V.S., Geeurickx, E., Declerck, C., Duskunovic, N., De Sutter, D., Noppen, S., Delport, F., Schols, D., Swinnen, J.V., Eyckerman, S., Hendrix, A., Lammertyn, J., Spasic, D., 2021. FO-SPR biosensor calibrated with recombinant extracellular vesicles enables specific and sensitive detection directly in complex matrices. J Extracell Vesicles 10(4), e12059.

Yoshioka, Y., Kosaka, N., Konishi, Y., Ohta, H., Okamoto, H., Sonoda, H., Nonaka, R., Yamamoto, H., Ishii, H., Mori, M., Furuta, K., Nakajima, T., Hayashi, H., Sugisaki, H., Higashimoto, H., Kato, T., Takeshita, F., Ochiya, T., 2014. Ultra-sensitive liquid biopsy of circulating extracellular vesicles using ExoScreen. Nat Commun 5, 3591.

Zendrini, A., Paolini, L., Busatto, S., Radeghieri, A., Romano, M., Wauben, M.H.M., van Herwijnen, M.J.C., Nejsum, P., Borup, A., Ridolfi, A., Montis, C., Bergese, P., 2019. Augmented COlorimetric NANoplasmonic (CONAN) Method for Grading Purity and Determine Concentration of EV Microliter Volume Solutions. Front Bioeng Biotechnol 7, 452.

Zeng, R., Wang, J., Wang, Q., Tang, D., Lin, Y., 2021. Horseradish peroxidase-encapsulated DNA nanoflowers: An innovative signal-generation tag for colorimetric biosensor. Talanta 221, 121600.

Zhang, H., Wang, Z., Wang, F., Zhang, Y., Wang, H., Liu, Y., 2020a. In Situ Formation of Gold Nanoparticles Decorated Ti3C2 MXenes Nanoprobe for Highly Sensitive Electrogenerated Chemiluminescence Detection of Exosomes and Their Surface Proteins. Anal Chem 92(7), 5546-5553.

Zhang, H., Wang, Z., Zhang, Q., Wang, F., Liu, Y., 2019. Ti3C2 MXenes nanosheets catalyzed highly efficient electrogenerated chemiluminescence biosensor for the detection of exosomes. Biosens Bioelectron 124-125, 184-190.

Zhang, J., Zhu, Y., Shi, J., Zhang, K., Zhang, Z., Zhang, H., 2020b. Sensitive Signal Amplifying a Diagnostic Biochip Based on a Biomimetic Periodic Nanostructure for Detecting Cancer Exosomes. ACS Appl Mater Interfaces 12(30), 33473-33482.

Zhang, P., He, M., Zeng, Y., 2016. Ultrasensitive microfluidic analysis of circulating exosomes using a nanostructured graphene oxide/polydopamine coating. Lab Chip 16(16), 3033-3042.

Zhang, P., Wu, X., Gardashova, G., Yang, Y., Zhang, Y., Xu, L., Zeng, Y., 2020c. Molecular and functional extracellular vesicle analysis using nanopatterned microchips monitors tumor progression and metastasis. Sci Transl Med 12(547).

Zhang, Y., Jiao, J., Wei, Y., Wang, D., Yang, C., Xu, Z., 2020d. Plasmonic Colorimetric Biosensor for Sensitive Exosome Detection via Enzyme-Induced Etching of Gold Nanobipyramid@MnO2 Nanosheet Nanostructures. Anal Chem 92(22), 15244-15252.

Zhang, Y., Su, Q., Song, D., Fan, J., Xu, Z., 2021. Label-free detection of exosomes based on ssDNA-modulated oxidase-mimicking activity of CuCo2O4 nanorods. Anal Chim Acta 1145, 9-16.

Zhang, Y., Wang, F., Zhang, H., Wang, H., Liu, Y., 2019b. Multivalency Interface and g-C3N4 Coated Liquid Metal Nanoprobe Signal Amplification for Sensitive Electrogenerated Chemiluminescence Detection of Exosomes and Their Surface Proteins. Anal Chem 91(18), 12100-12107.

Zhao, X., Zhang, W., Qiu, X., Mei, Q., Luo, Y., Fu, W., 2020. Rapid and sensitive exosome detection with CRISPR/Cas12a. Anal Bioanal Chem 412(3), 601-609.

Zhao, Z., Yang, Y., Zeng, Y., He, M., 2016. A microfluidic ExoSearch chip for multiplexed exosome detection towards blood-based ovarian cancer diagnosis. Lab Chip 16(3), 489-496.

Zhou, Q., Rahimian, A., Son, K., Shin, D.S., Patel, T., Revzin, A., 2016a. Development of an aptasensor for electrochemical detection of exosomes. Methods 97, 88-93.

Zhou, Y., Xu, H., Wang, H., Ye, B.C., 2019a. Detection of breast cancer-derived exosomes using the horseradish peroxidase-mimicking DNAzyme as an aptasensor. Analyst 145(1), 107-114.

Zhou, Y.G., Mohamadi, R.M., Poudineh, M., Kermanshah, L., Ahmed, S., Safaei, T.S., Stojcic, J., Nam, R.K., Sargent, E.H., Kelley, S.O., 2016b. Interrogating Circulating Microsomes and Exosomes Using Metal Nanoparticles. Small 12(6), 727-732.

Zhou, Z., Wu, Q., Yan, Z., Zheng, H., Chen, C.J., Liu, Y., Qi, Z., Calandrelli, R., Chen, Z., Chien, S., Su, H.I., Zhong, S., 2019b. Extracellular RNA in a single droplet of human serum reflects physiologic and disease states. Proc Natl Acad Sci U S A 116(38), 19200-19208.

Zhu, F., Li, D., Ding, Q., Lei, C., Ren, L., Ding, X., Sun, X., 2020. 2D magnetic MoS2-Fe3O4 hybrid nanostructures for ultrasensitive exosome detection in GMR sensor. Biosens Bioelectron 147, 111787.

Zhu, L., Wang, K., Cui, J., Liu, H., Bu, X., Ma, H., Wang, W., Gong, H., Lausted, C., Hood, L., Yang, G., Hu, Z., 2014. Label-free quantitative detection of tumor-derived exosomes through surface plasmon resonance imaging. Anal Chem 86(17), 8857-8864.

Zhu, N., Li, G., Zhou, J., Zhang, Y., Kang, K., Ying, B., Yi, Q., Wu, Y., 2021. A light-up fluorescence resonance energy transfer magnetic aptamer-sensor for ultra-sensitive lung cancer exosome detection. J Mater Chem B 9(10), 2483-2493.

Zhu, S., Li, H., Yang, M., Pang, S.W., 2018. Highly sensitive detection of exosomes by 3D plasmonic photonic crystal biosensor. Nanoscale 10(42), 19927-19936.

List of tables

Table 1 – Summarized description of optical methods for biosensing EVs.

Detection method	Sample	LOD	Ref
Fluorescence detection			
Fluorophore and quencher -"Turn-on" strategy, using fluorescently labelled anti-CD63 on the surface of MoS$_2$-CNT	Cell culture media	1.48×10^3 particles μL^{-1}	**(Tayebi et al. 2019)**
-"Turn-on" strategy, using fluorescently labelled and GO as a quencher	Cell culture media	3.43×10^5 particles μL^{-1}	**(Li et al. 2020)**
-"Turn-off" strategy, using imprinted cavities formed with exosomes and fluorescent markers	Cell culture media	6 pg mL^{-1}	**(Mori et al. 2019)**
Amplification based on nanostructures -Copper-mediated signal amplification	Serum	4.8×10^4 particles μL^{-1}	**(He et al. 2018)**
-Encapsulation of a fluorescent substance in magnetic nanobeads	Serum	-	**(Kabe et al. 2019)**
-Plasmonic metallic nanostructures-based signal amplification	Cell culture media	-	**(Min et al. 2020)**
-Quantum dots-based signal amplification	Cell culture media	5×10^2 particles μL^{-1}	**(Wu et al. 2021)**
Rolling circle amplification -Initiation of RCA after recognition of exosomes by a DNA primer comprising an aptamer	Cell culture media	1×10^2 particles μL^{-1}	**(Huang et al. 2018)**
-Based on branched RCA and an aptamer to target specific exosomes	Cell culture media	42.7 particles μL^{-1}	**(Huang et al. 2020b)**
Amplification based on DNA walker -Recyclable 3D multipedal DNA walker triggered by the presence of exosomes	Cell culture media	1 particle μL^{-1}	**(Wang et al. 2020b)**
Amplification based on CRISPR system -Triggering of CRISPR/Cas12a system by exosomes, leading to the release of a fluorescent label	Cell culture media	-	**(Zhao et al. 2020)**
Microfluidic devices -Microfluidic platform with GO and polydopamine nanointerface	Cell culture media	50 exosomes μL^{-1}	**(Zhang et al. 2016)**
-ExoSearch chip for multiplexed exosome detection	Plasma	7.5×10^2 particles μL^{-1}	**(Zhao et al. 2016)**

-Power-free PDMS microchip using laminar flow-assisted dendritic amplification	Cell culture media	-	**(Ishihara et al. 2017)**
-3D nanopatterned microchips	Cell culture media	16 EVs µL^{-1}	**(Zhang et al. 2020c)**
Electrochemiluminescence detection			
-ECL probes based on Graphite-like carbon nitride nanosheets conjugated polydopamine coated galinstan NPs	Cell culture media	31 particles µL^{-1}	**(Zhang et al. 2019b)**
- ECL probes based on Ti$_3$C$_2$ MXenes nanosheets	Cell culture media	1.25×10^2 particles µL^{-1}	**(Zhang et al. 2019a)**
-ECL probes based on Ti$_3$C$_2$ MXenes and AuNPs	Cell culture media	30 particles µL^{-1}	**(Zhang et al. 2020a)**
SPR detection			
Versatility of SPR biosensors design -Measurement of optical transmission through periodic nanoholes on a metal surface	Cell culture media	3×10^3 exosomes	**(Im et al. 2014)**
-TiN as a biocompatible plasmonic material, instead of gold or silver	Cell culture media	4.29×10^{-3} µg mL^{-1} (for CD63) 2.75×10^{-3} µg mL^{-1} (for EGFRvIII)	**(Qiu et al. 2019)**
-Fibre optic SPR platform	Cell culture media and plasma	-	**(Yildizhan et al. 2021)**
Signal amplification -Amplification of the SPR signal using DNA hydrogel functionalized AuNPs	Cell culture media	10^2 particles µL^{-1}	**(Chen et al. 2020b)**
Microarrays -Combination of SPR imaging with antibody microarrays	Cell culture media	-	**(Zhu et al. 2014)**
Differentiation between EVs - Localized SPR biosensor with self-assembly gold nanoislands to distinguish between exosomes and microvesicles	Cell culture media	0.194 µg mL^{-1} (for exosomes)	**(Thakur et al. 2017)**
- Detection of multiple exosome subpopulations	Plasma	1 µg mL^{-1}	**(Picciolini et al. 2018)**
-Differentiation between normal and cancerous cells	Cell culture media	10^4 particles µL^{-1}	**(Fan et al. 2020)**
SERS detection			
Label-free methods	Cell culture media	-	**(Tirinato et al. 2012)**

-Super-hydrophobic micropillars to concentrate the target and enhance the SERS signal			
-Nanobowl-structured plasmonic substrates to capture and detect exosomes	Cell culture media	1 exosome per nanobowl	**(Lee et al. 2015a)**
-Combination of silver nanocubes on a surface with gold nanorods	Cell culture media	-	**(Sivashanmugan et al. 2017)**
-Attachment of AuNPs directly to the EVs, followed by overgrowing them with a silver layer *in situ*	Cell culture media	-	**(Fraire et al. 2019)**
-Microscale biosilicate substrate embedded with silver nanoparticles	Cell culture media	0.6 particles μL^{-1}	**(Rojalin et al. 2020)**
-Macroporous inverse opal to capture and analyse exosomes	Plasma	-	**(Dong et al. 2020)**
-Combination of plasmonic nanobowties and microfluidics	Cell culture media	1.32×10^2 particles μL^{-1}	**(Jalali et al. 2021)**
Label-dependent methods -SERS and fluorescent nanotags	Cell culture media	2×10^3 exosomes μL^{-1}	**(Kwizera et al. 2018)**
-Immunomagnetic capture of exosomes and SERS nanoprobes	Cell culture media	27 particles μL^{-1}	**(Tian et al. 2018)**
-Bimetallic SERS-active nanotags	Cell culture media	26 particles μL^{-1}	**(Ning et al. 2020)**

Colorimetric detection

Particles aggregation -Colour change due to AuNPs aggregation	Serum	-	**(Maiolo et al. 2015)**
-Colour change due to AuNPs aggregation	Cell culture media	-	**(Jiang et al. 2017)**
Catalytic reactions -pH strips adapted to exosomes detection	Cell culture media	4.46×10^3 particles μL^{-1}	**(Yang et al. 2019)**
-Enzyme-induced etching of gold nanobipyramid@MnO2 nanostructures	Cell culture media	1.35×10^2 particles μL^{-1}	**(Zhang et al. 2020d)**
-Enzymatic catalysis of dopamine in the presence of exosomes	Cell culture media	7.7 particles μL^{-1}	**(Xu et al. 2020)**
Lateral flow immunochromatographic strips -Sandwich system based on tetraspanin antibodies immobilized on the strip and AuNPs-conjugated antibodies	Cell culture media	8.54×10^5 exosomes μL^{-1}	**(Oliveira-Rodriguez et al. 2016)**

-System based on carbon-coated superparamagnetic nanoflowers	Plasma	4×10^6 EVs µL^{-1}	**(Moyano et al. 2020)**
DNA-assisted amplification			
-Triggering DNA-assisted amplification by target-induced proximity ligation	Cell culture media	0.1 particles µL^{-1}	**(Liu et al. 2018b)**
Photonic detection			
Plasmonic effect			
-3D plasmonic PC nanostructures with point-defect cavities	Cell culture media	-	**(Zhu et al. 2018)**
Photonic and fluorescence			
-Integrated chip with a double-filtration unit and detection using PCs and fluorescence	Cell culture media	8.9 EVs µL^{-1}	**(Dong et al. 2019b)**
-Signal amplification based on PCs and quantum dots	Cell culture media	-	**(Zhang et al. 2020b)**
Microfluidic devices			
-Differentiation between host and parasitic EVs	Cell culture media	2.18×10^6 EVs µL^{-1}	**(Wang et al. 2018a)**

Table 2 – Summarized description of electrochemical, magnetic and piezoelectric biosensors for EVs detection.

Detection method	Sample	LOD	Ref
Electrochemical detection			
Sandwich- type immunoassay			
-Capture of exosomes with CD9 antibodies and detection with IgG antibodies conjugated to HRP	Cell culture media	2×10^2 exosomes μL^{-1}	**(Doldan et al. 2016)**
-Capture of exosomes with CD9 antibodies and detection using antibodies against HER-2	Cell culture media	4.7×10^5 exosomes μL^{-1}	**(Yadav et al. 2017)**
-Combined enzymatic reaction with a redox cycling on nanointerdigitated electrodes	Cell culture media	5 EVs μL^{-1}	**(Mathew et al. 2020)**
Nanoparticle-labelling			
-Functionalized AgNPs and CuNPs to recognize exosomal surface markers	Cell culture media	50 exosomes per sensor	**(Zhou et al. 2016b)**
-COFs-based nanoprobe with AuNPs functionalized with a linker and HRP	Cell culture media	1.60×10^2 particles μL^{-1}	**(Wang et al. 2020d)**
Microfluidic devices			
-Incorporation of gold electrodes into a microfluidic system and displacement of probing strands	Cell culture media	1×10^3 particles μL^{-1}	**(Zhou et al. 2016a)**
-Aptasensor assisted by a DNA nanotetrahedron structure	Cell culture media	20.9 exosomes μL^{-1}	**(Wang et al. 2017a)**
-Aptasensor combined with a vortex-type microfluidic device	Cell culture media	17 particles μL^{-1}	**(Kashefi-Kheyrabadi et al. 2020)**
DNA amplification strategies			
-Specific aptamers to gastric cancer exosomes and RCA	Cell culture media	0.954 exosomes μL^{-1}	**(Huang et al. 2019)**
-Aptamers specific to breast cancer exosomes and amplification with multidirectional hybridization chain reaction	Cell culture media	2.85×10^2 exosomes μL^{-1}	**(Wang et al. 2021a)**
Magnetic separation and electrochemical detection			
-Induced multi-DNA release and cyclic enzymatic amplification	Cell culture media	70 particles μL^{-1}	**(Dong et al. 2018)**
-Magnetic enrichment combined with an aptasensor on ITO electrode	Cell culture media	4.39 particles μL^{-1}	**(Xu et al. 2018)**
Magnetic detection			

-Microfluidic chip with magnetic separation and detection using a micro nuclear magnetic resonance system	Cell culture media and blood	-	**(Shao et al. 2012)**
-Magnetoresistive biosensor chip	Cell culture media	10^5 microvesicles μL^{-1}	**(Cherré et al. 2017)**
-On-chip GMR biosensor for EVs detection and profiling of surface glycans	Cell culture media	10^4 EVs	**(Wang et al. 2020g)**
-GMR biosensor based on MoS_2–Fe_3O_4 probes	Cell culture media	10^2 exosomes	**(Zhu et al. 2020)**
Piezoelectric detection			
Acoustic-based technique -AuNPs-amplified SAW sensor	Cell culture media	1.1 particles μL^{-1}	**(Wang et al. 2020a)**
QCM-based technique -QCM system functionalized with anti-CD63	Spiked serum	2.9×10^5 exosomes μL^{-1} (frequency response) 1.4×10^5 exosomes μL^{-1} (dissipation response)	**(Suthar et al. 2020)**
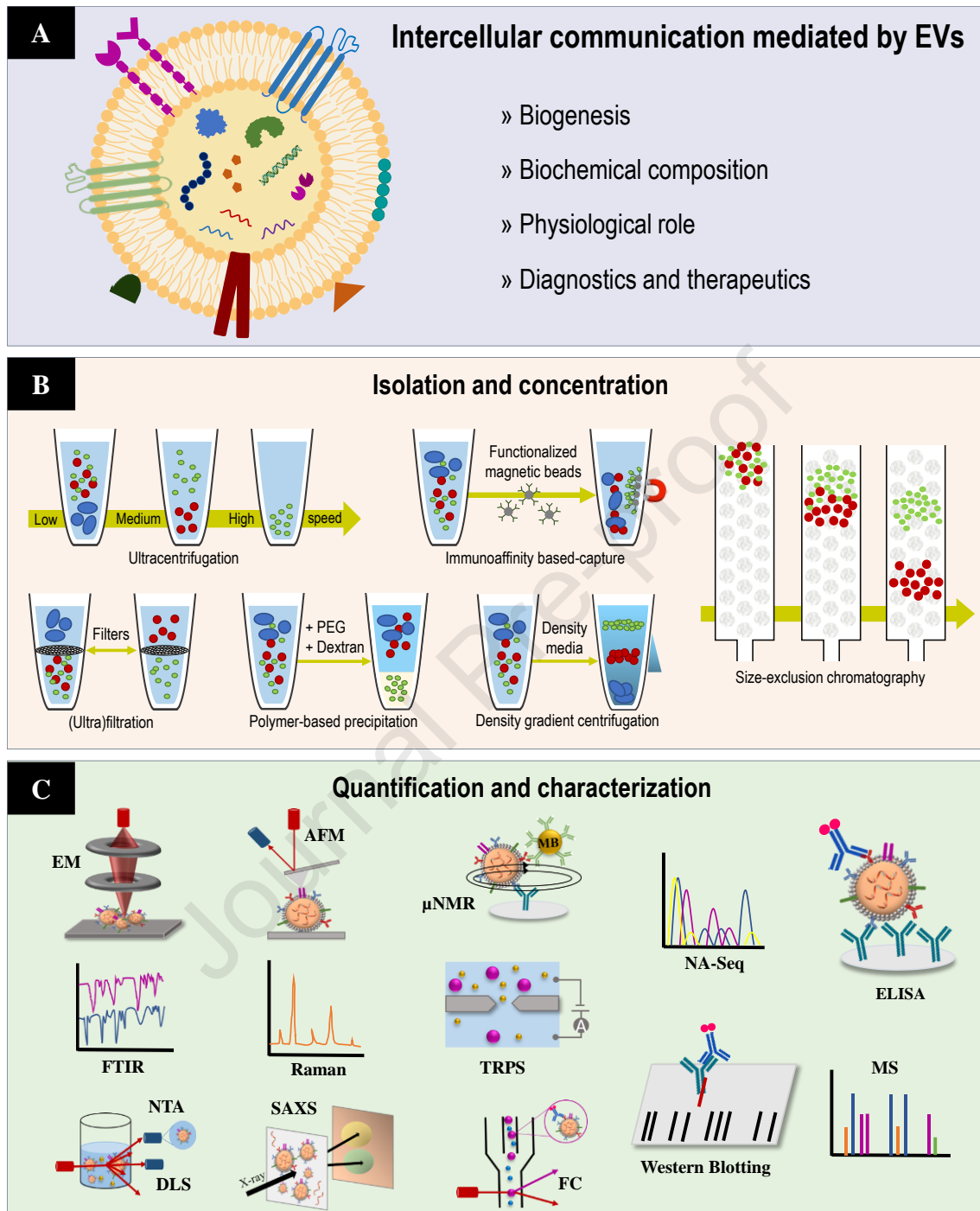
Fig. 1 – **(A)** Schematic representation of EVs whose content biomarkers have been studied in complementary research fields; **(B)** Commonly used standard isolation and concentration methods; **(C)** Physicochemical and biochemical methods used for quantification and characterization of EVs (EM – electron microscopy; AFM – atomic force microscopy; μNMR – micro nuclear magnetic resonance; FTIR – Fourier- transform infrared spectroscopy; TRPS –

tunable resistive pulse sensing; NTA – nanoparticle tracking analysis; DLS – dynamic light scattering ; SAXS – small angle X-ray scattering; FC – flow cytometry ; NA-Seq – nucleic acids sequencing; ELISA – enzyme-linked immunosorbent protein assays; MS – mass spectrometry).
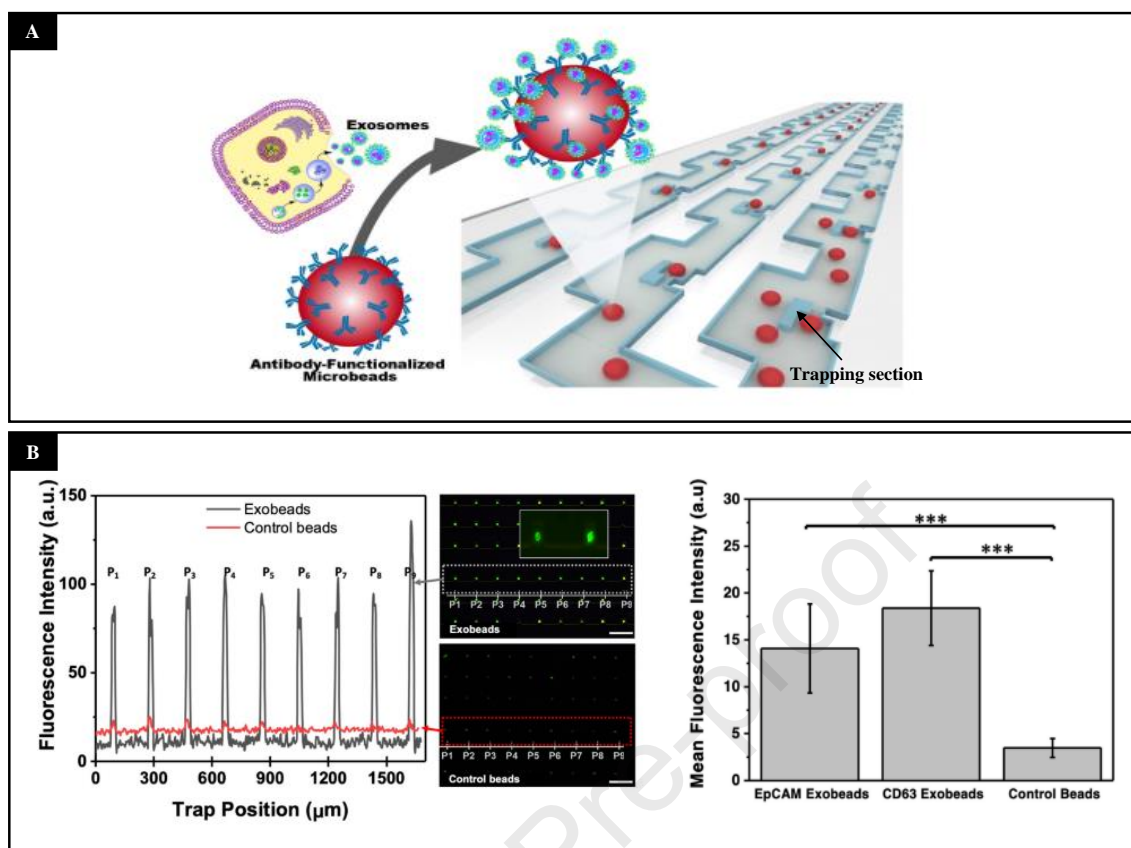
Fig. 2 – (A) Schematic diagram of the trapping microchannels of the immunoaffinity-based separation microfluidic device. It used microbeads functionalized with CD63 antibody or EpCAM for the specific isolation of exosomes. **(B)** Analysis of the efficiency of exosomes capture through quantification of the fluorescence intensity of the differently modified microbeads, Copyright 2020, American Chemical Society; Reproduced with permission (Tayebi et al. 2020).
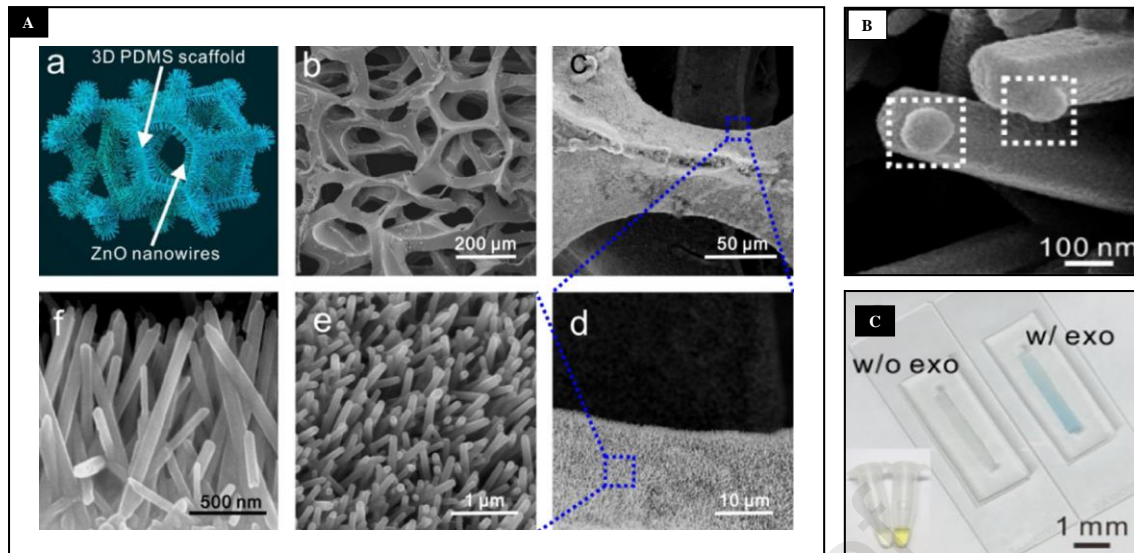
Fig. 3 – (A) Illustration of the ZnO nanowires 3D scaffold (a), and SEM images of the scaffold with increasing magnification (b-f). **(B)** SEM image of the exosomes captured on ZnO nanowires, and **(C)** their colorimetric detection, Copyright 2018, Elsevier; Reproduced with permission (Chen et al. 2018).
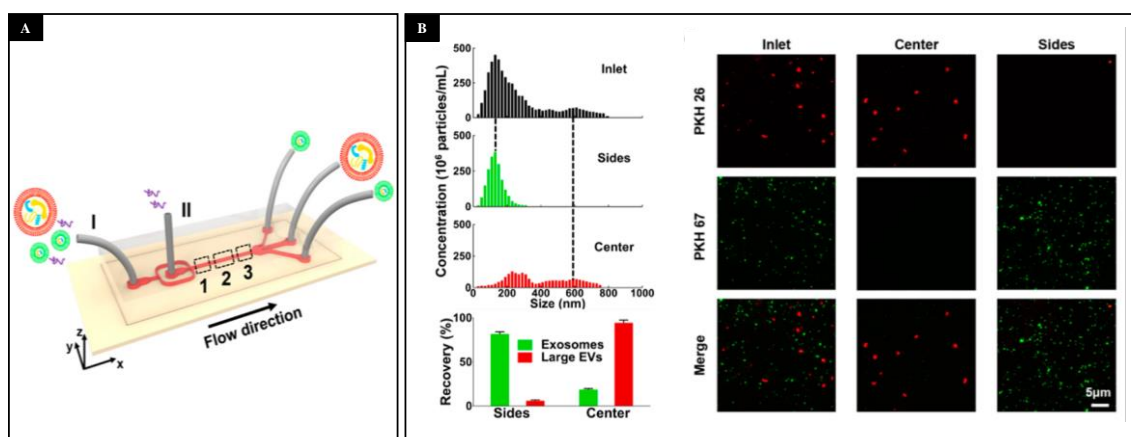
Fig. 4 – (A) Schematic representation of the microfluidic chip for exosome separation from large EVs based on viscoelastic flow. The collection of exosomes occurs at the two side outlets, whereas large EVs are collected in the middle outlet. **(B)** Characterization of the separation based on NTA and fluorescence images. Exosomes were prelabelled with PKH26 dye (green colour), while large EVs were prelabelled with PKH67 dye (red colour), Copyright 2017, American Chemical Society; Reproduced with permission (Liu et al. 2017).
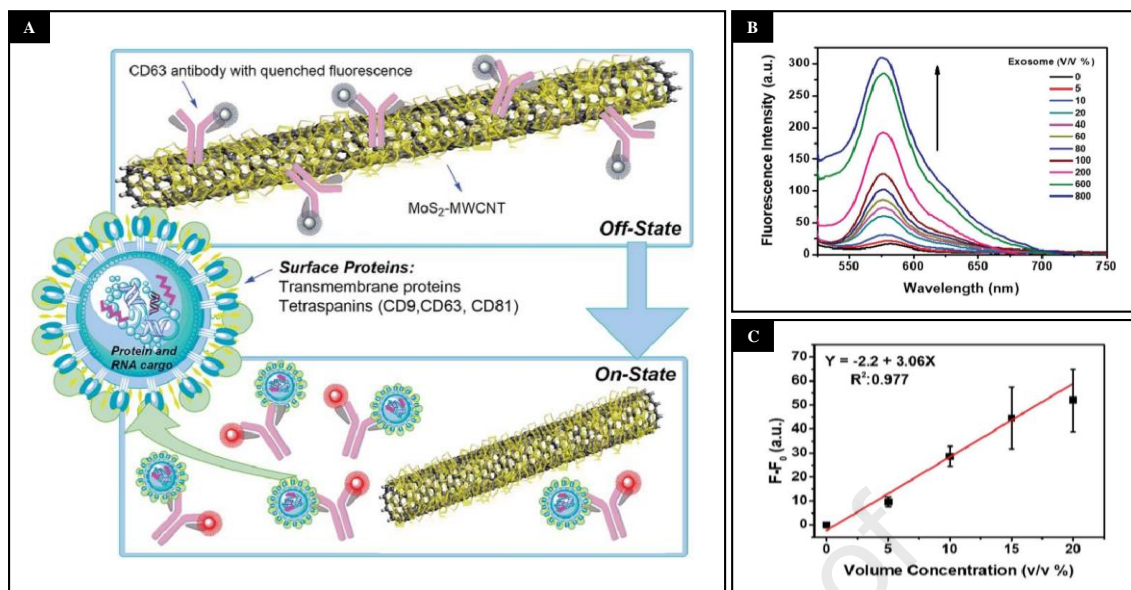
Fig. 5 – (A) Schematic representation of fluorescently labelled anti-CD63 on the surface of MoS$_2$-multiwall carbon nanotubes, which act as a fluorescent quenching material. **(B)** Exosome detection based on fluorescence recovery and **(C)** calibration curve, Copyright 2019, Royal Society of Chemistry; Reproduced under the terms and conditions of the Creative Commons Attribution 3.0 Unported License (Tayebi et al. 2019).
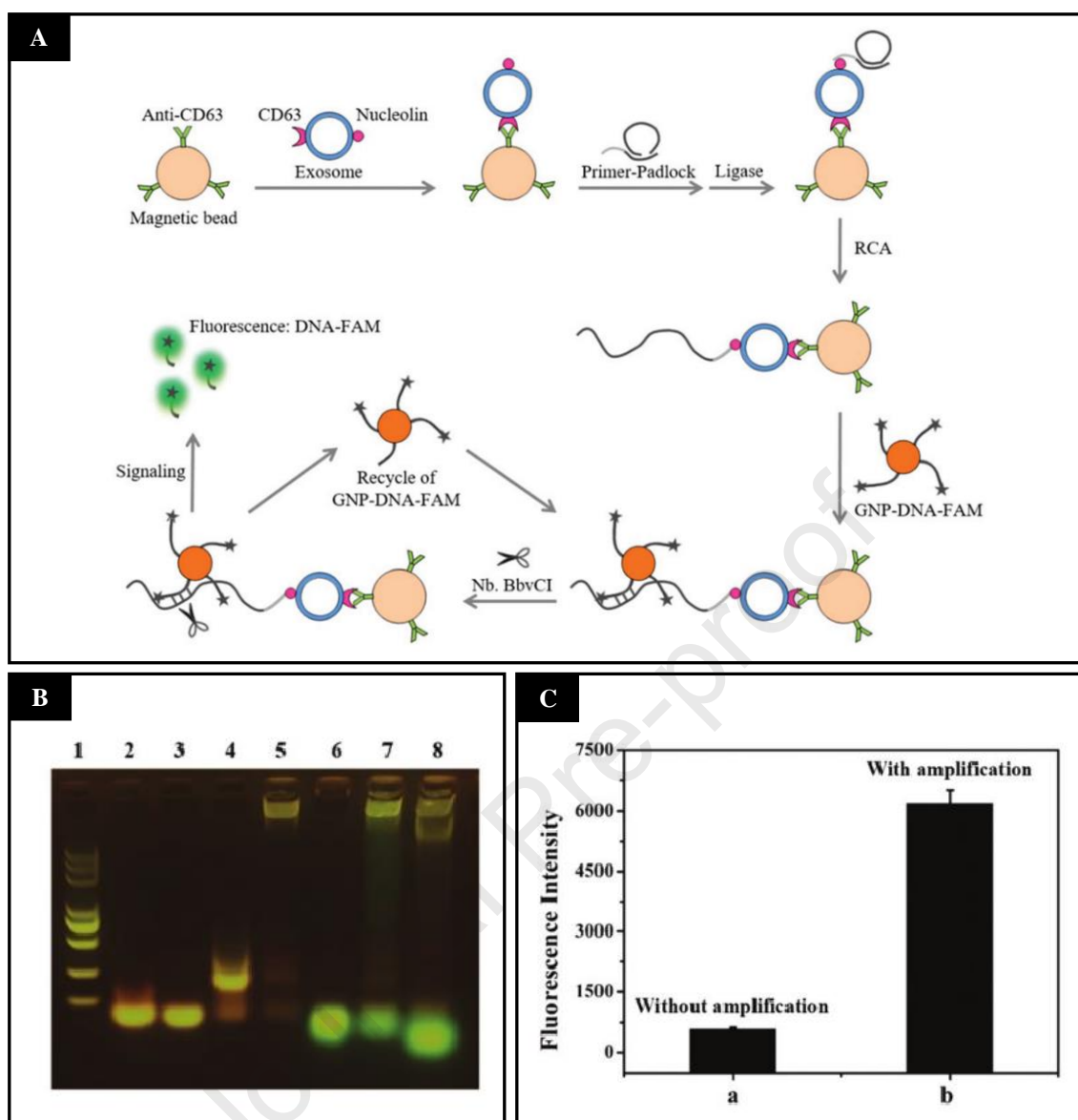
Fig. 6 – (A) Illustration of the rolling circle amplification (RCA)-based platform for the detection of leukaemia-derived exosomes, and **(B)** RCA products. Lane 1: marker; Lane 2: primer; Lane 3: padlock; Lane 4: primer + padlock; Lane 5: RCA products; Lane 6: DNA–FAM (DNA primer connected to a fluorescent dye); Lane 7: RCA products + DNA–FAM; Lane 8: RCA products + DNA–FAM + Nb·BbvCI nicking endonuclease. **(C)** Confirmation of the increased intensity of the signal with the amplification technique employed Copyright 2018, Royal Society of Chemistry; Reproduced under the terms and conditions of the Creative Commons Attribution 3.0 Unported License (Huang et al. 2018).
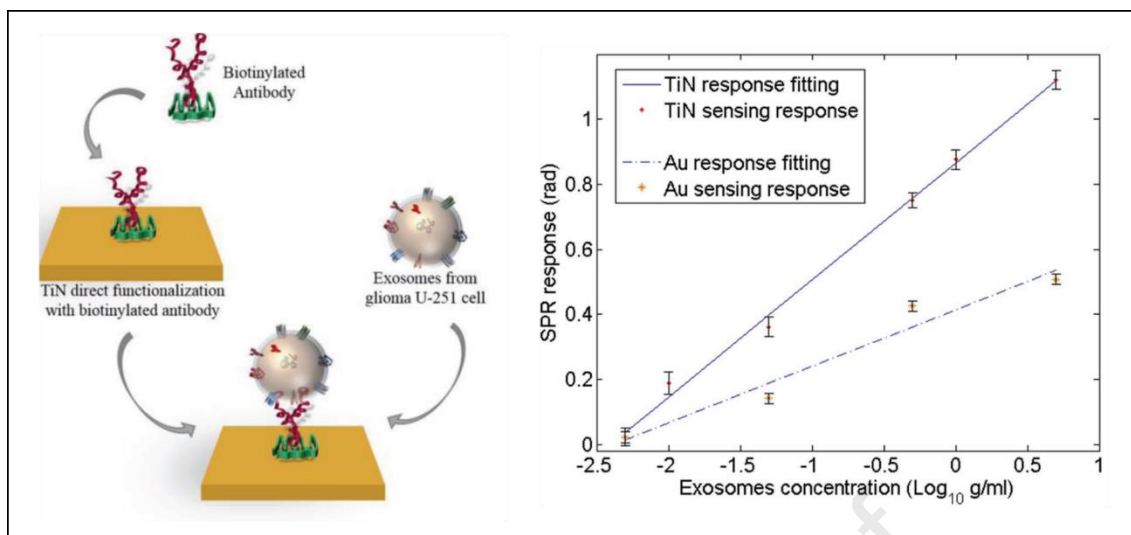
Fig. 7 – Scheme of the TiN SPR biosensor and comparison between TiN and Au SPR responses for the detection of glioma-derived exosomes, Copyright 2018, Wiley-VCH; Reproduced with permission (Qiu et al. 2019).
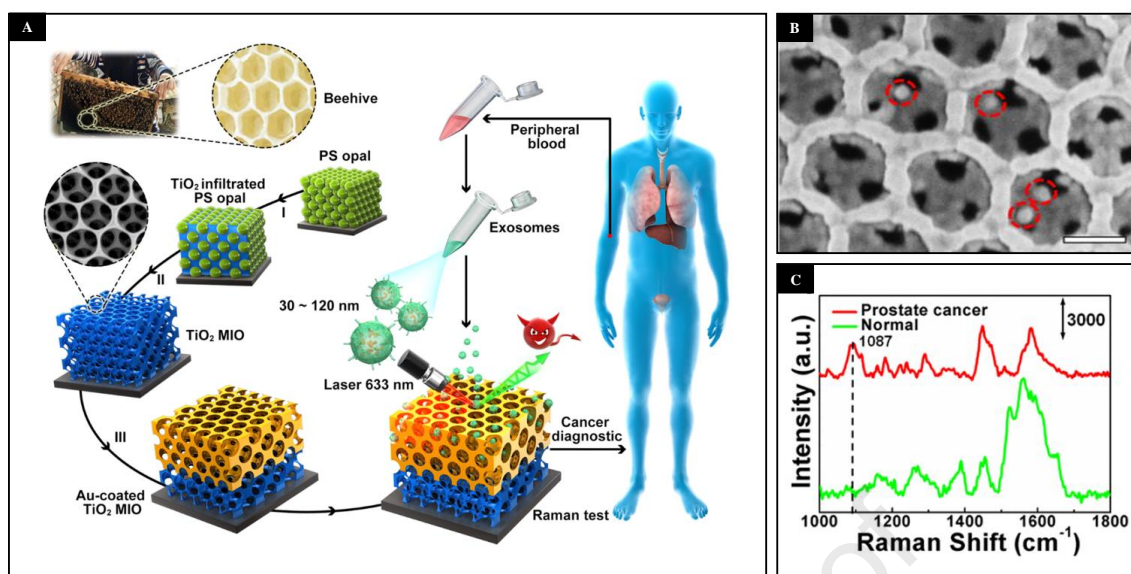
Fig. 8 – (A) Diagram of the design and detection based on the macroporous inverse opal structure and **(B)** SEM image of the captured exosomes (scale bar: 300 nm). **(C)** SERS spectra obtained for exosomes from plasma of a healthy individual and of a prostate cancer patient, Copyright 2020, American Chemical Society; Reproduced with permission (Dong et al. 2020).
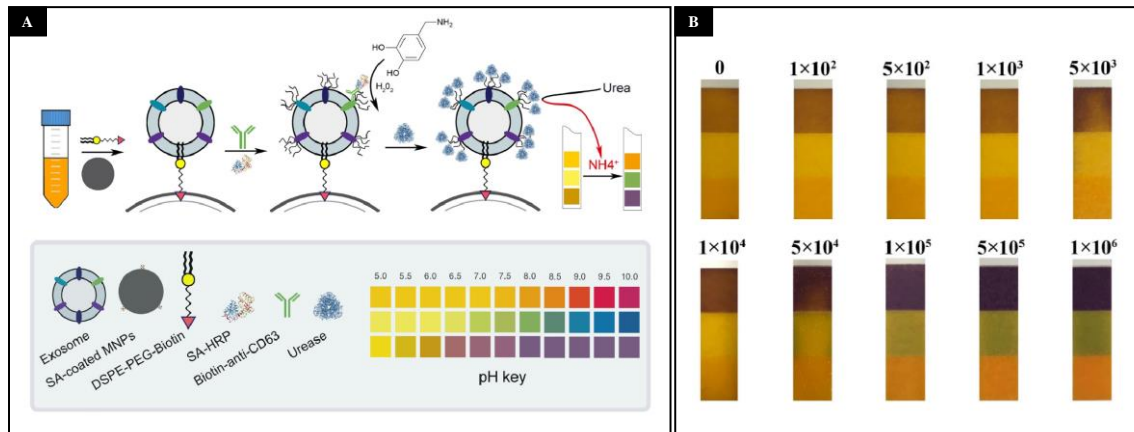
Fig. 9 – (A) Schematic representation of a novel system created for exosomes detection and quantification based on commercially available pH strips. After isolation of exosomes with magnetic nanoparticles (MNPs), antibodies against CD63 (biotin-anti-CD63) conjugated with horseradish peroxidase (SA-HRP) catalyse the formation of a polydopamine film on exosomes surface, which in turn allows the binging of urease. By adding urea to the system, urease converts it into ammonia and the pH increases. **(B)** The pH variation is related to exosomes concentration, what is noticeable in pH strips by colour change, Copyright 2019, Elsevier; Reproduced with permission (Yang et al. 2019).
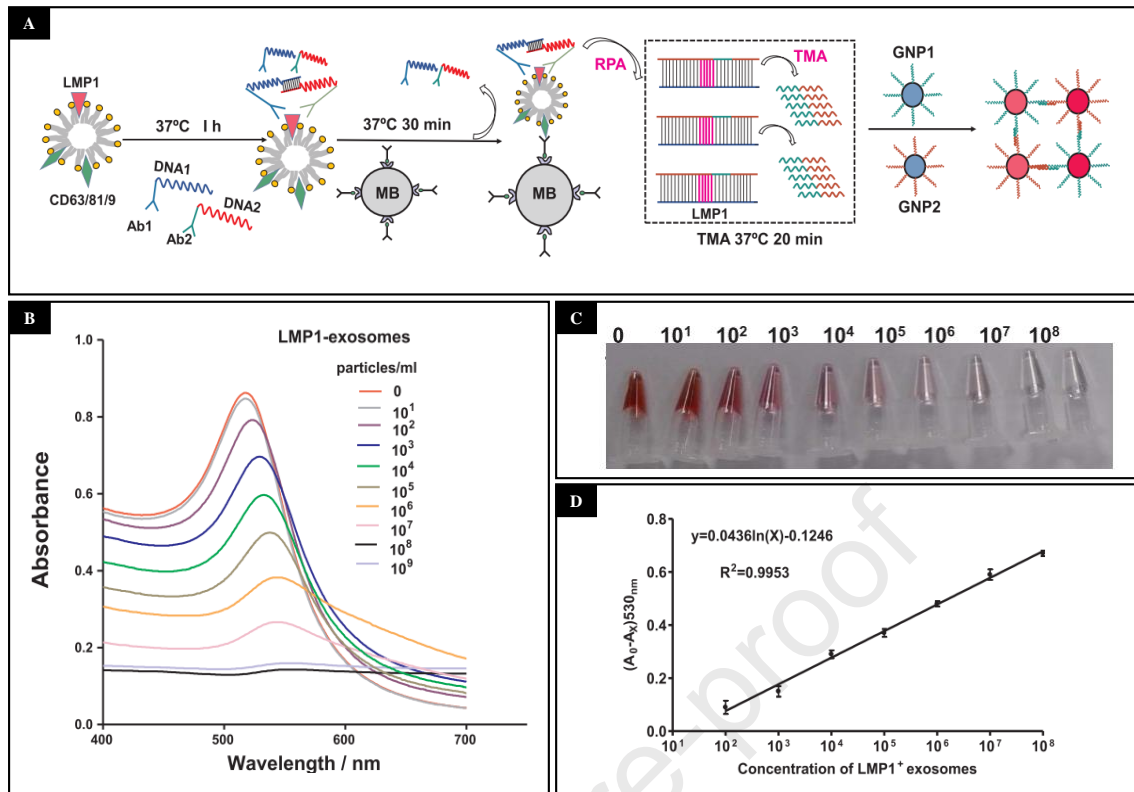
Fig. 10 – (A) Diagram representing the colorimetric technique used to detect LMP1$^+$ exosomes.
(B) Absorbance spectra of different concentrations of exosomes, and corresponding **(C)** colour images and **(D)** calibration curve, Copyright 2018, Elsevier; Reproduced with permission (Liu et al. 2018b).
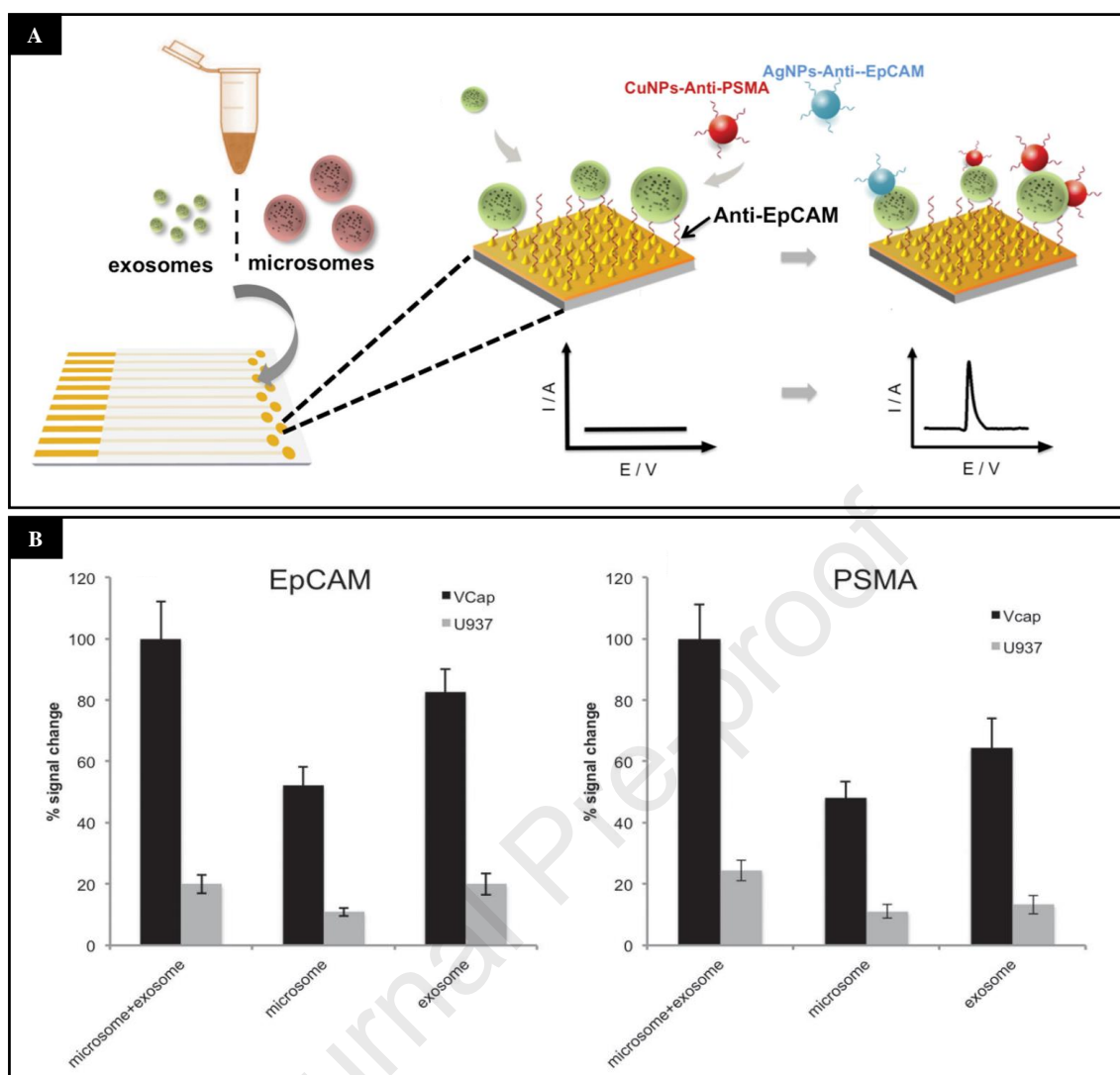
Fig. 11 – (A) Scheme regarding the operation principle of the electrochemical biosensor for the analysis of exosomes and microsomes. **(B)** Electrochemical assay for the detection of fractions containing microsomes and exosomes, microsomes only, or exosomes only, isolated from VCaP cell culture supernatant using AgNPs–anti-EpCAM and CuNPs–anti-PSMA as markers. The U937 cell line is a nonepithelial cell line, used as a control in the assays, Copyright 2016, Wiley; Reproduced with permission (Zhou et al. 2016b).
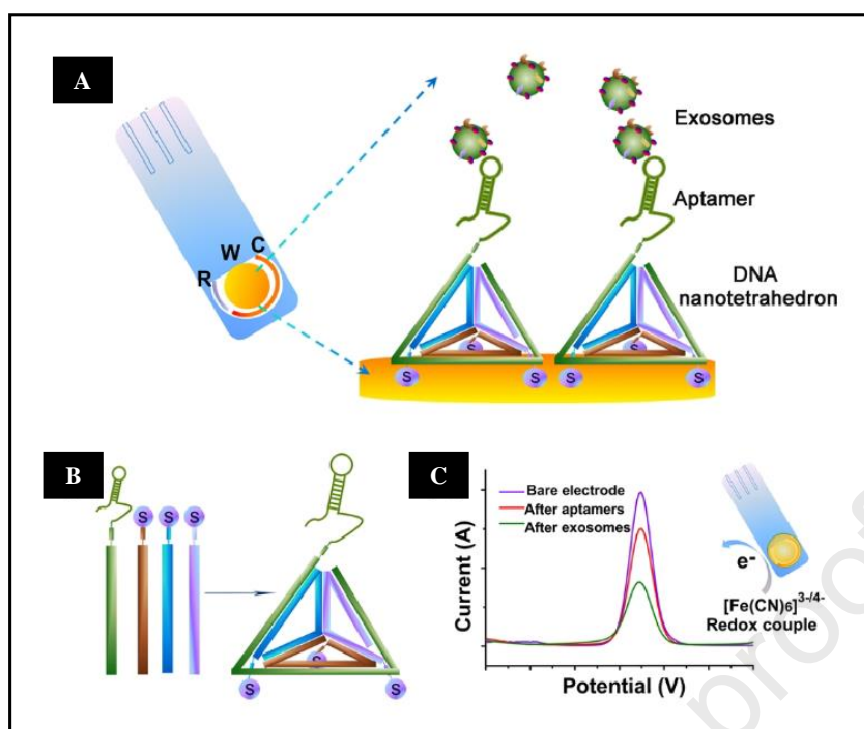
Fig. 12 – (A) Scheme of the electrochemical device, which used **(B)** DNA nanotetrahedron structure for assisting the aptamer to detect and capture exosomes from hepatocarcinoma cells; **(C)** Redox signal changes after aptamer immobilization and after incubation with exosomes, Copyright 2017, American Chemical Society; Reproduced with permission (Wang et al 2017a).
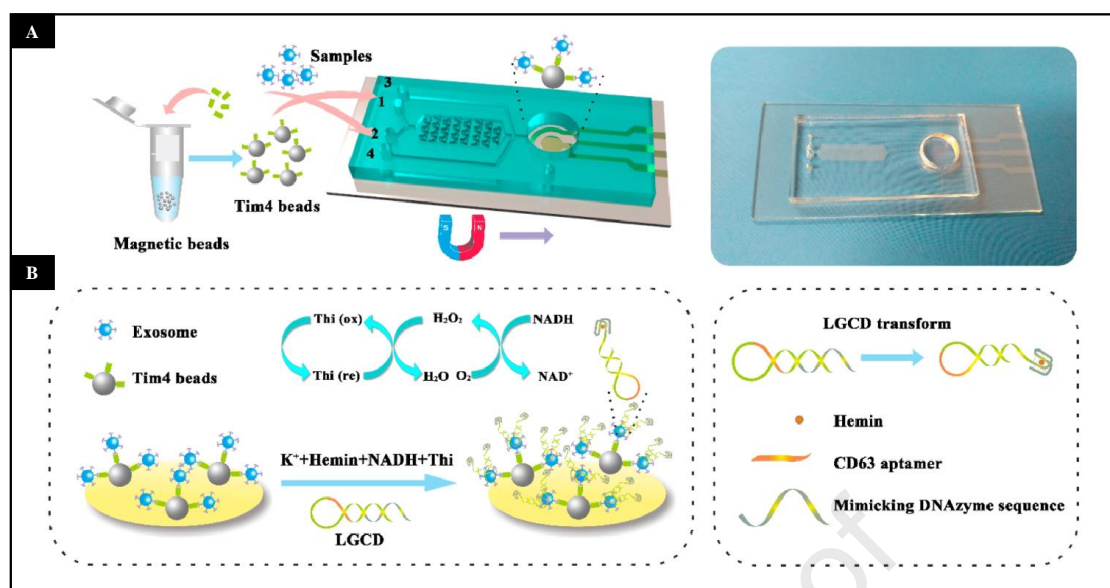
Fig. 13 – (A) The first stage of this microfluidic system corresponds to the isolation process: Y-shaped micropillars were patterned for anisotropic flow of the sample, and binding of exosomes to phosphatidylserine-Tim4 protein enriched magnetic nanoparticles. **(B)** The second stage reports to the ITO electrode containing a CD63 aptamer and a G-rich mimicking DNAzyme sequence. In the presence of exosomes, the single-stranded DNA hairpin is opened and forms a G-quadruplex that in coordination with hemin leads to NADH oxidation, which in turns leads to a measurable electrochemical signal, Copyright 2018, American Chemical Society; Reproduced with permission (Xu et al. 2018).
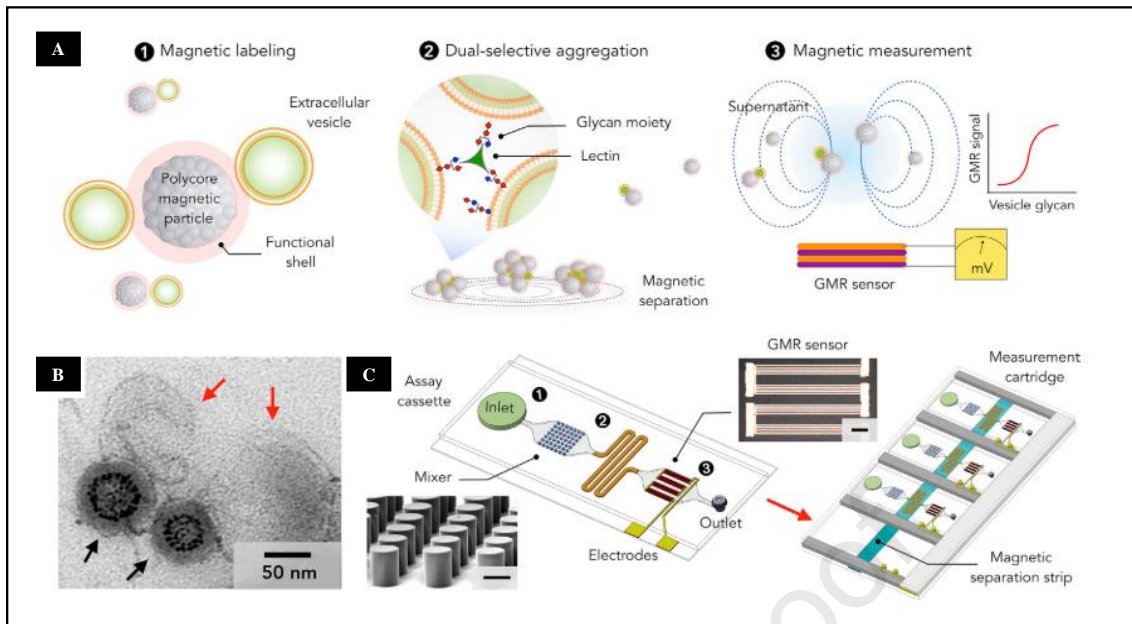
Fig. 14 – (A) Schematic representation of the magnetic device operation, based on three functional steps: magnetic labelling, dual-selective aggregation and EVs quantification through a GMR sensor. **(B)** Transmission electron micrograph of EVs bound to the magnetic particles. **(C)** Schematic of the multiplex platform, Copyright 2020, Elsevier; Reproduced with permission (Wang et al. 2020g).
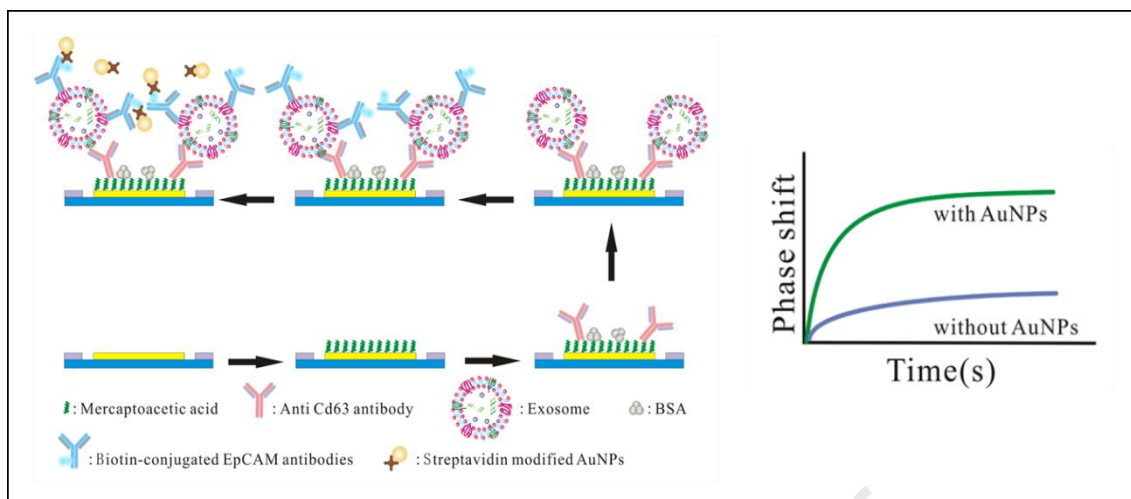
Fig. 15 – Schematic illustration of an acoustic biosensor for the detection of exosomes, with signal amplification based on AuNPs, Copyright 2020, American Chemical Society; Reproduced with permission (Wang et al. 2020a).

Porto, 9th of December of 2021

Highlights

Breaking the classics: next-generation biosensors for the isolation, profiling and detection of extracellular vesicles

➢ Extracellular vesicles (EVs) as important members of cell signaling

➢ Biomolecules in EVs may function as disease biomarkers

➢ Conventional methods for monitoring biomarkers in EVs

➢ Biosensing methods for monitoring biomarkers in EVs

➢ Successful application to wine sample analysis, in line with the sensory panel.

Breaking the classics: next-generation biosensors for the isolation, profiling and detection of extracellular vesicles

Raquel Vaz, Verónica M. Serrano, Yuselis Castaño-Guerrero, Ana Rita Cardoso, Manuela F. Frasco and M. Goreti F. Sales

Declaration of interests

☒ The authors declare that they have no known competing financial interests or personal relationships that could have appeared to influence the work reported in this paper.

☐ The authors declare the following financial interests/personal relationships, which may be considered as potential competing interests:

The authors,

Raquel Vaz
Verónica Serrano
Yuselis Castaño-Guerrero
Ana Rita Cardoso
Manuela Frasco
Goreti Sales